



Research paper

Novel iodoacetamido benzoheterocyclic derivatives with potent antileukemic activity are inhibitors of STAT5 phosphorylation



Romeo Romagnoli ^{a,*}, Pier Giovanni Baraldi ^a, Filippo Prencipe ^a, Carlota Lopez-Cara ^a, Riccardo Rondanin ^a, Daniele Simoni ^a, Ernest Hamel ^b, Stefania Grimaudo ^c, Rosaria Maria Pipitone ^c, Maria Meli ^d, Manlio Tolomeo ^e

^a Dipartimento di Scienze Chimiche e Farmaceutiche, Università di Ferrara, 44121 Ferrara, Italy

^b Screening Technologies Branch, Developmental Therapeutics Program, Division of Cancer Treatment and Diagnosis, Frederick National Laboratory for Cancer Research, National Cancer Institute, National Institutes of Health, Frederick, MD 21702, USA

^c Dipartimento Biomedico di Medicina Interna e Specialistica, Università di Palermo, 90125 Palermo, Italy

^d Dipartimento di Scienze per la Promozione della Salute e Materno Infantile, Area di Farmacologia, Università di Palermo, 90125 Palermo, Italy

^e Centro Interdipartimentale di Ricerca in Oncologia Clinica e Dipartimento Biomedico di Medicina Interna e Specialistica, Sezione di Malattie Infettive, Università di Palermo, 90125 Palermo, Italy

ARTICLE INFO

Article history:

Received 28 September 2015

Received in revised form

6 November 2015

Accepted 16 November 2015

Available online xxx

Keywords:

STAT5 inhibitors

BCR/ABL expressing leukemia

Apoptosis

Structure-activity relationship

In vitro antiproliferative activity

ABSTRACT

Signal Transducer and Activator of Transcription 5 (STAT5) protein, a component of the STAT family of signaling proteins, is considered to be an attractive therapeutic target because of its involvement in the progression of acute myeloid leukemia. In an effort to discover potent molecules able to inhibit the phosphorylation-activation of STAT5, twenty-two compounds were synthesized and evaluated on the basis of our knowledge of the activity of 2-(3',4',5'-trimethoxybenzoyl)-3-iodoacetamido-6-methoxy benzo[b]furan derivative **1** as a potent STAT5 inhibitor. Most of these molecules, structurally related to compound **1**, were characterized by the presence of a common 3',4',5'-trimethoxybenzoyl moiety at the 2-position of different benzoheterocycles such as benzo[b]furan, benzo[b]thiophene, indole and *N*-methylindole. Effects on biological activity of the iodoacetamido group and of different moieties (methyl and methoxy) at the C-3 to C-7 positions were examined. In the series of benzo[b]furan derivatives, moving the iodoacetyl amino group from the C-4 to the C-5 or C-6 positions did not significantly affect antiproliferative activity. Compounds **4**, **15**, **20** and **23** blocked STAT5 signals and induced apoptosis of K562 BCR–ABL positive cells. For compound **23**, the trimethoxybenzoyl moiety at the 2-position of the benzo[b]furan core was not essential for potent inhibition of STAT5 activation.

© 2015 Elsevier Masson SAS. All rights reserved.

1. Introduction

The ultimate goal of research in cancer therapy is to develop treatments that specifically target the cancer cell while leaving normal cells intact. The introduction of the BCR–ABL tyrosine kinase inhibitor imatinib in chronic myelogenous leukemia (CML) therapy has been a major advance in leukemia treatment [1–3]. However, clinical drug resistance often can develop through the acquisition of BCR–ABL gene mutations, which make this oncoprotein refractory to inhibition by imatinib or other tyrosine kinase inhibitors, such as nilotinib and dasatinib. In addition, BCR–ABL

independent mechanisms of resistance were also described [4–6]. Therefore, the hunt for better effective agents is ongoing.

The identification of novel compounds modulating the expression/activity of molecular targets downstream to BCR–ABL could be a new approach in the treatment of CML resistant to BCR–ABL targeted molecules. In fact, the mechanism through which BCR–ABL contributes to malignant transformation is dependent from the ability of this oncoprotein to activate a variety of signaling pathways and downstream targets such as STAT5, RAS, phosphatidylinositol-3'-kinase (PI3K), and others [7–10]. Many studies have shown that constitutive activation of the gene Signal Transducers and Activators of Transcription 5 (STAT5) plays an important role in the pathogenesis of CML induced by BCR–ABL [11–14], as well as in acute myeloid leukemias (AML) [15–17] and in polycythemia rubra vera [18,19]. STAT5 is the component of a family of seven proteins

* Corresponding author.

E-mail address: rmr@unife.it (R. Romagnoli).

(STAT1–6) critical for the pathogenesis of many tumors [20–22], but these proteins are largely dispensable in normal adult cells [23], suggesting that they could be targets with a high therapeutic index [24–26]. STAT proteins transduce signals from the cell surface to the nucleus, where they regulate the expression of genes that control proliferation, survival, self-renewal, and other critical cellular functions [27]. Under normal physiological conditions, the activation of STATs is tightly regulated. In cancer, by contrast, STAT proteins, particularly STAT3 and STAT5 [28], become activated constitutively, thereby driving the malignant phenotype of cancer cells [29–32].

In order to be functional, STAT5 protein must first be activated. This activation is carried out by kinases associated with transmembrane receptors at the cell surface. First, ligands (cytokines, growth factors) binding to these transmembrane receptors on the outside of the cell activate Janus kinase 2 (JAK2), which in turn adds a phosphate group to a specific tyrosine residue on the receptor. STAT5 then binds to these phosphorylated-tyrosines using their SH2 domain. The bound STAT5 is then phosphorylated by JAK2, and the phosphorylated STAT5 (pSTAT5) finally goes on to form either homodimers, STAT5–STAT5, or heterodimers, STAT5–STATX with other STAT proteins [33,34]. The STAT5 dimer then translocates to the nucleus, where STAT5 binds to a consensus DNA sequence and promotes expression of specific STAT5 target genes (e.g., Bcl-xl, c-Myc, *pim*-1, p21, MCL-1, Osm and JAB).

Differently from normal cells, in which STAT5 is activated by JAK2, in CML the product of the fusion protein BCR–ABL directly activates the STAT5 protein. Activated STAT5 seems to play a crucial role in growth and survival of CML cells, suggesting that drugs able to inhibit STAT5 activation could be useful for the treatment of this type of leukemia, especially for CML resistant to BCR–ABL targeted molecules [35]. However, despite many years of intensive research devoted to the discovery of small molecules targeting STAT5, none of the direct inhibitors of STAT5 [36–42] have been approved for clinical use in oncology.

Previously we synthesized a new series of 2-(3',4',5'-trimethoxybenzoyl)-3-amino-benzo[*b*]furan compounds that showed cytotoxic activity in BCR–ABL expressing cells [43]. Among them, we identified the 2-(3',4',5'-trimethoxybenzoyl)-3-iodoacetamido-6-methoxybenzo[*b*]furan derivative **1** (TR120) as a potent inducer of apoptosis in the BCR–ABL-positive K562 and KCL-22 cell lines and in their imatinib resistant counterpart K562-R and KCL22-R cells *in vitro* (Chart 1). Compound **1** induced a marked decrease in the pSTAT5 level in these cell lines, along with a block of cells in G1, a decrease in cyclin D expression and an increase in the percentage of apoptotic cells [44]. Preliminary structure-activity relationship (SAR) analysis indicated that the iodoacetamido function at the C-3 position of the benzo[*b*]furan ring system was essential for STAT5 inhibitory activity, while the corresponding bromoacetyl amino and chloroacetyl amino analogs were inactive. The activity of compound **1** as a STAT5 inhibitor caused us to undertake a further SAR study, by the design and synthesis of different series of derivatives. All the synthesized compounds were characterized by the presence of an electrophilic iodoacetamido function that can potentially react with essential thiol groups in the STAT5 functional domains and thus alter their function.

By the preparation of the corresponding isomeric analogs **2** and **3**, which retain the iodoacetyl amino moiety at the C-3 position of 2-(3',4',5'-trimethoxybenzoyl)benzo[*b*]furan skeleton, we turned our attention to the position of the methoxy group, by moving it to either the C-5 or C-7 position of the benzo[*b*]furan system, respectively. Compound **4** was unsubstituted on the benzene portion of the benzo[*b*]furan ring. Since the iodoacetyl amino had proved to be favorable for activity, through the synthesis of compounds **5–12** we investigated the effect on biological activity of

moving the iodoacetyl amino function from the 3 to the 4, 5, 6 or 7-position of the 2-(3',4',5'-trimethoxybenzoyl)benzo[*b*]furan nucleus. Finally, we prepared a set of 2-(3',4',5'-trimethoxybenzoyl)benzoheterocyclic derivatives structurally related to **1**, obtained by replacing the original benzo[*b*]furan nucleus with various bioisosteric benzoheterocycles such as indole (**13**), *N*-methylindole (**14**, **15**) and benzo[*b*]thiophene (**16–20**). Besides the methoxy group, another substituent examined was the weak electron-donating methyl substituent in the benzene portion of the benzo[*b*]heterocyclic system. Since the 3,4,5-trimethoxyphenyl group is found in many antitubulin compounds, such as colchicine, podophyllotoxin and combretastatin A-4 (CA-4) [45], by the synthesis of compounds **21–23** we investigated the influence of the 3,4,5-trimethoxybenzoyl group at the 2-position of the 3-iodoacetyl amino benzo[*b*]furan derivative **4** on STAT5 inhibitory activity, by the substitution of this moiety with a 3,4-dimethoxybenzoyl (**21**), 4-methoxybenzoyl (**22**) or benzoyl (**23**) group.

2. Chemistry

The synthesis of eight of the twenty-two compounds (**2–4** and **16–20**) was previously described by our research group [46]. The new iodoacetyl amino benzo[*b*]furan derivatives **5–12** and **21–23** as well as the iodoacetamido indole analogs **13–15** were synthesized following the procedure described in Scheme 1. The acylation of amino benzo[*b*]furans **24–31** and **35–37** or amino indoles **32–34** [47] with bromoacetyl bromide in CH₂Cl₂ furnished the desired bromoacetamido intermediate **38–45**, **49–51** and **46–48**, respectively. The final iodo derivatives **5–15** and **21–23** were obtained from the corresponding bromo intermediates **38–51** through an exchange reaction using sodium iodide in *N,N*-dimethylacetamide at room temperature.

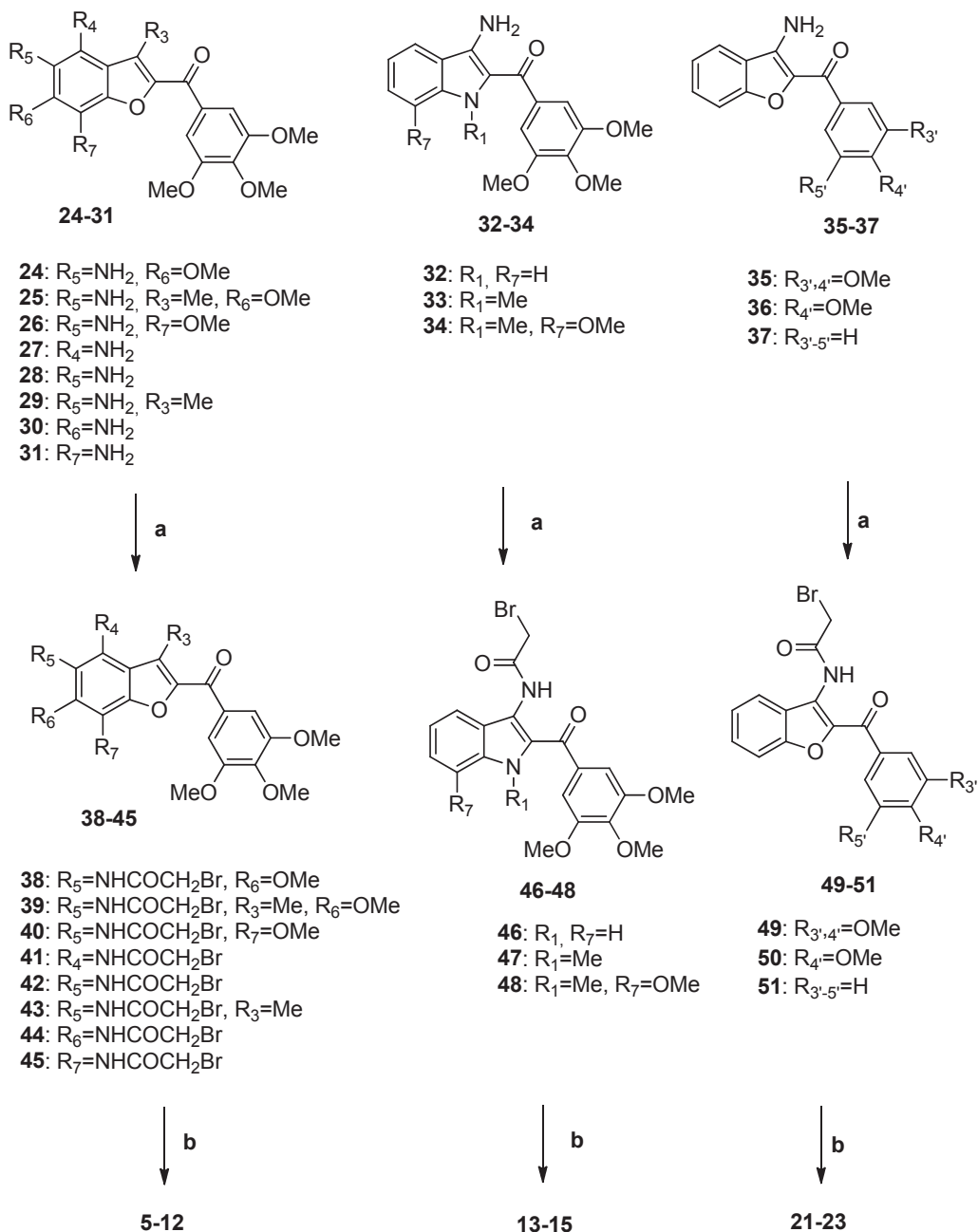
3. Biological results

3.1. *In vitro* cytotoxic activity

Table 1 shows the cytotoxic effects evaluated as IC₅₀ (concentration able to inhibit cell growth by 50%) and AC₅₀ (concentration able to induce apoptosis in 50% of the cells) of iodoacetamido derivatives **2–23** against K562 cells exposed to each derivative for 48 h, using analog **1** and imatinib mesilate as reference compounds. As shown in Table 1, the IC₅₀ values of the new series ranged from 0.07 to 18 μM, and the AC₅₀ values ranged from 0.2 to 48 μM (except for compound **12**, which was inactive at 50 μM). Out of the twenty-two derivatives, twelve (**4–9**, **11**, **13**, **15**, **17**, **18** and **20**) exhibited good activity with IC₅₀ values lower than 1.0 μM.

The most active cytotoxic agent identified in this study was the 2-(3',4',5'-trimethoxybenzoyl)-3-methyl-5-(iodoacetyl amino)-6-methoxybenzo[*b*]furan derivative **6**, which showed an IC₅₀ 1.8- and 3.1-fold lower than those of the reference derivatives **1** and imatinib, respectively. As an apoptotic agent, **6** was 1.8- and 2.7- times more active than **1** and imatinib, respectively. Compound **6** differed from **1** in the position of the iodoacetamido group and from compound **5**, which had the iodoacetamido group in the same position as **6**, in having a methyl substituent at position 3. It should be noted that, simply moving the iodoacetamido group, resulted in a 3.3-fold loss in antiproliferative activity, comparing the IC₅₀ obtained with **5** versus that obtained with **1**.

For the 3-iodoacetamido benzo[*b*]furan derivatives **1–3**, a comparison of substituent effect revealed that the cytotoxic activity was dependent on the methoxy substitution and on its location on the benzene portion of the benzo[*b*]furan moiety, with the most favorable position being C-6 (reference compound **1**). The IC₅₀



Scheme 1. Reagents and conditions. a: BrCH_2COBr , Py, CH_2Cl_2 , rt, 1 h; b: NaI, $\text{CH}_3\text{CON}(\text{CH}_3)_2$, rt, 18 h.

obtained with **1** exceeded that obtained with the C-5 or C-7 methoxy counterparts **2** and **3** by more than one and two-orders of magnitude, respectively. A 7.5-fold reduction of activity was also observed following removal of the C-6 methoxy group of **1**, to furnish derivative **4**.

The IC_{50} and AC_{50} values obtained showed that the position of iodoacetyl amino group on the benzo[*b*]furan system greatly affected antiproliferative activity, with the C-7 iodoacetyl amino derivative **12** being inactive ($\text{IC}_{50} > 50 \mu\text{M}$), while the C-3, C-4, C-5 and C-6 iodoacetamido derivatives **4**, **8**, **9** and **11**, respectively, had comparable activity, with IC_{50} values ranging from 0.6 to 0.9 μM . These compounds all differed from **1**, in addition, by the absence of a methoxy substituent on the benzo[*b*]furan moiety. The activity of the 5-iodoacetamido derivative **9** was 30-fold reduced by the

introduction of a methyl group at the C-3 position of benzo[*b*]furan nucleus (compound **10**). However, this methyl substituent was also present, along with the 6-methoxy group, in the most active agent in the series, compound **6**, while only the 6-methoxy yielded the less active compound **5**.

Comparing derivatives **5** and **9** with their 3-methyl congeners **6** and **10**, respectively, the introduction of a methyl at the C-3 position of compound **5** increased antiproliferative and apoptotic activity 6- and 8-fold, while an opposite effect was observed for compound **9**, in which the C-3 methyl substitution produce a 30- and 10-fold reduction in cell growth inhibition and apoptotic potency, respectively.

Comparing the C-3 iodoacetamido derivatives without substituents on the benzene portion of benzoheterocyclic system (**4**,

Table 1
Antiproliferative (IC₅₀) and apoptotic (AC₅₀) effects of compounds **2**–**23** evaluated in K562 cells after a 48 h treatment.

Compounds	IC ₅₀ (μM) ^a	AC ₅₀ (μM) ^b
1	0.12 ± 0.03	0.45 ± 0.05
2	3.2 ± 0.3	7.8 ± 0.9
3	14 ± 2.2	24 ± 2.8
4	0.9 ± 0.3	6.5 ± 0.7
5	0.4 ± 0.07	2 ± 0.6
6	0.07 ± 0.008	0.25 ± 0.05
7	0.4 ± 0.06	2.2 ± 0.4
8	0.8 ± 0.18	4.5 ± 0.6
9	0.6 ± 0.08	2.9 ± 0.3
10	18 ± 4	26.8 ± 5.3
11	0.6 ± 0.08	2.9 ± 0.3
12	>50	>50
13	0.5 ± 0.06	2.4 ± 0.2
14	4.3 ± 0.3	8.2 ± 1.4
15	0.8 ± 0.12	4.6 ± 0.7
16	18 ± 4	28 ± 4.8
17	0.8 ± 0.2	4.2 ± 0.7
18	0.78 ± 0.09	3.7 ± 0.5
19	1 ± 0.3	4.7 ± 0.5
20	0.4 ± 0.08	2.8 ± 0.3
21	22 ± 3.3	48 ± 6.7
22	2.9 ± 0.1	6.8 ± 0.7
23	1 ± 0.3	5.9 ± 0.8
Imatinib	0.22 ± 0.04	0.68 ± 0.08

Data are expressed as the mean ± SE from the dose-response curves of at least two to three independent experiments.

^a Concentration able to inhibit cell growth by 50%.

^b Concentration able to induce apoptosis in 50% of cells.

13, **14** and **16**), activity increased with indole (**13**) > benzo[*b*]furan (**4**) > *N*-methylindole (**14**) >> benzo[*b*]thiophene (**16**), with IC₅₀ values of 0.5, 0.9, 4.3 and 18 μM, and AC₅₀ values of 2.4, 6.5, 8.2 and 28 μM, respectively. While the *N*-methylindole derivative **14** was 8-fold less active in comparison with the *N*-unsubstituted congener **13** (IC₅₀: 4.3 and 0.5 μM, respectively), a 5-fold improvement in antiproliferative activity (IC₅₀ = 0.8 μM) was observed for the parent compound **15**, obtained by the introduction of a methoxy group at the C-7 position of the *N*-methylindole nucleus of **14**. From the SAR point of view, replacing benzo[*b*]furan with benzo[*b*]thiophene (compound **16**) increased IC₅₀ and AC₅₀ values 20- and 4.3-fold as compared with **4**, indicating that sulfur and oxygen atoms are not bioequivalent when the iodoacetylamino moiety was located at the C-3 position, while the corresponding C-5 iodoacetylamino benzo[*b*]furan and benzo[*b*]thiophene isomers **9** and **17**, respectively, showed similar antiproliferative and apoptotic activities. The data also indicated that the introduction of the weak electron-releasing methyl group at the C-6 position of **16**, to afford the derivative **19**, resulted in a marked increase of the cytotoxic and apoptotic activity. Moreover, shifting the methyl substitution to C-7, as in compound **20**, further enhanced potency, with **20** 2.5-fold more active than **19** (IC₅₀ = 0.4 and 1.0 μM, respectively; AC₅₀ = 2.8 and 4.7 μM, respectively).

Returning to the benzo[*b*]thiophene derivatives, for compound **16**, the least active in the group, simply moving the iodoacetylamino group from the C-3 to the C-5 position, to furnish derivative **17**, led to a 22.5- and 6.7-fold increase in the cell growth inhibition and apoptotic activities. In addition, compound **18**, bearing a methoxy substituent at the C-7 position, had activity similar to that of both **17** and **19**, but this activity was 2-fold lower than that of the corresponding benzo[*b*]furan analog **7**. In the benzo[*b*]thiophene group, the most active compound was **20**, with a methyl substituent at position 3 (about twice as active as compounds **18** and **19**, with a methoxy at position 7 or a methyl at position 6, respectively).

In a comparison of the cytotoxic and apoptotic activities of

compounds **4** and **23**, we found that the replacement of the trimethoxybenzoyl with a benzoyl moiety (compounds **4** and **23**, respectively) maintained the IC₅₀ and AC₅₀ values, indicating that the trimethoxybenzene moiety was not required for activity in this compound class. However, both a single methoxy in the 4' position (**22**) and two methoxy groups at the 3' and 4' positions (**21**) led to small and large losses of activity, respectively, in comparison with compounds with either the trimethoxybenzene (**4**) or unsubstituted benzene (**23**).

3.2. Analysis of cell cycle effects and pSTAT5 expression

Once the antiproliferative activity was determined, we examined the influence of the most active compounds (showing an IC₅₀ ≤ 1 μM) on the cell cycle (Fig. 1, Table 2) and on pSTAT5 expression (Fig. 2, Table 3) in K562 cells. Analysis of cell cycle effects was carried out by flow cytometry after staining cells with propidium iodide; pSTAT5 expression was determined by flow cytometry after staining cells with a fluorochrome-conjugated anti-pSTAT5 monoclonal antibody. In Fig. 2, the curves expressing the fluorescence of cells stained with a fluoresceinated anti-pSTAT5 after a 24 h exposure to each compound (thick lines) were compared to those expressing the fluorescence of untreated cells stained with an anti-pSTAT5 (dotted lines) and to those stained with an isotype monoclonal antibody (thin lines). Although somewhat different multiples of the IC₅₀ values shown in Table 1 were used in the studies presented in Figs. 1 and 2, ranging from 1.9 for compound **7** to 7.1 for compound **6**, these concentrations were minimally cytotoxic at 24 h, as opposed to the 48 h used in the antiproliferative studies.

The most active antiproliferative molecule **6** (IC₅₀ = 0.07 μM; AC₅₀ = 0.25 μM) caused an increase in the percentage of cells in the G2M phase of cell cycle (Fig. 1d, Table 2), and morphological examination of treated cells showed most cells were blocked in metaphase (data not shown). These findings indicate that compound **6** acts in cells as an antimetabolic agent. Moreover, compound **6** was moderately active in decreasing the expression of activated STAT5 (pSTAT5) (Fig. 2c, Table 3; 44% inhibition relative to the untreated cells). Of interest, the two isomeric derivatives **5** and **7** (IC₅₀ = 0.4 μM; AC₅₀ = 2 μM) caused a modest increase in the proportion of cells in S phase and were unable (**7**) or only modestly able (**5**; 29% inhibition) to modify the expression of pSTAT5. In contrast, the benzo[*b*]thiophene derivative **20** induced a block of cells in G1 and a complete disappearance of activated pSTAT5 (Fig. 2m and Table 3). Compounds **9** (IC₅₀ = 0.6 μM; AC₅₀ = 2.9 μM) and **13** (IC₅₀ = 0.5 μM; AC₅₀ = 2.4 μM) induced modest decreases in pSTAT5 expression (19 and 30% inhibition, respectively) and also caused modest increases in the proportion of cells in S phase (Figs. 1g, i and 2f, h; Tables 2 and 3). Compounds **4**, **15**, **20** and **23** blocked cells in G1, and they were markedly active in modulating STAT5. Compound **19** showed effects on cell cycle and on pSTAT5 similar to those of **6**. Compounds **8**, **11** and **17** caused modest increases in the proportion of cells in the S phase and had only minimal effects on pSTAT5 levels, while compound **18** caused the greatest increase in cells in the G2M phase (Fig. 1j, Table 2) and modestly decreased pSTAT5 expression (Fig. 2k, Table 3; 36% inhibition).

3.3. Inhibition of tubulin polymerization and colchicine binding

To investigate whether STAT5 modulation was related to an interaction with tubulin, compounds **4**, **15**, **20** and **23**, the most active of the series in modulating STAT5, were selected to determine their inhibitory effects on tubulin polymerization and on the binding of colchicine to tubulin (Table 4). The benzo[*b*]thiophene derivative **20**

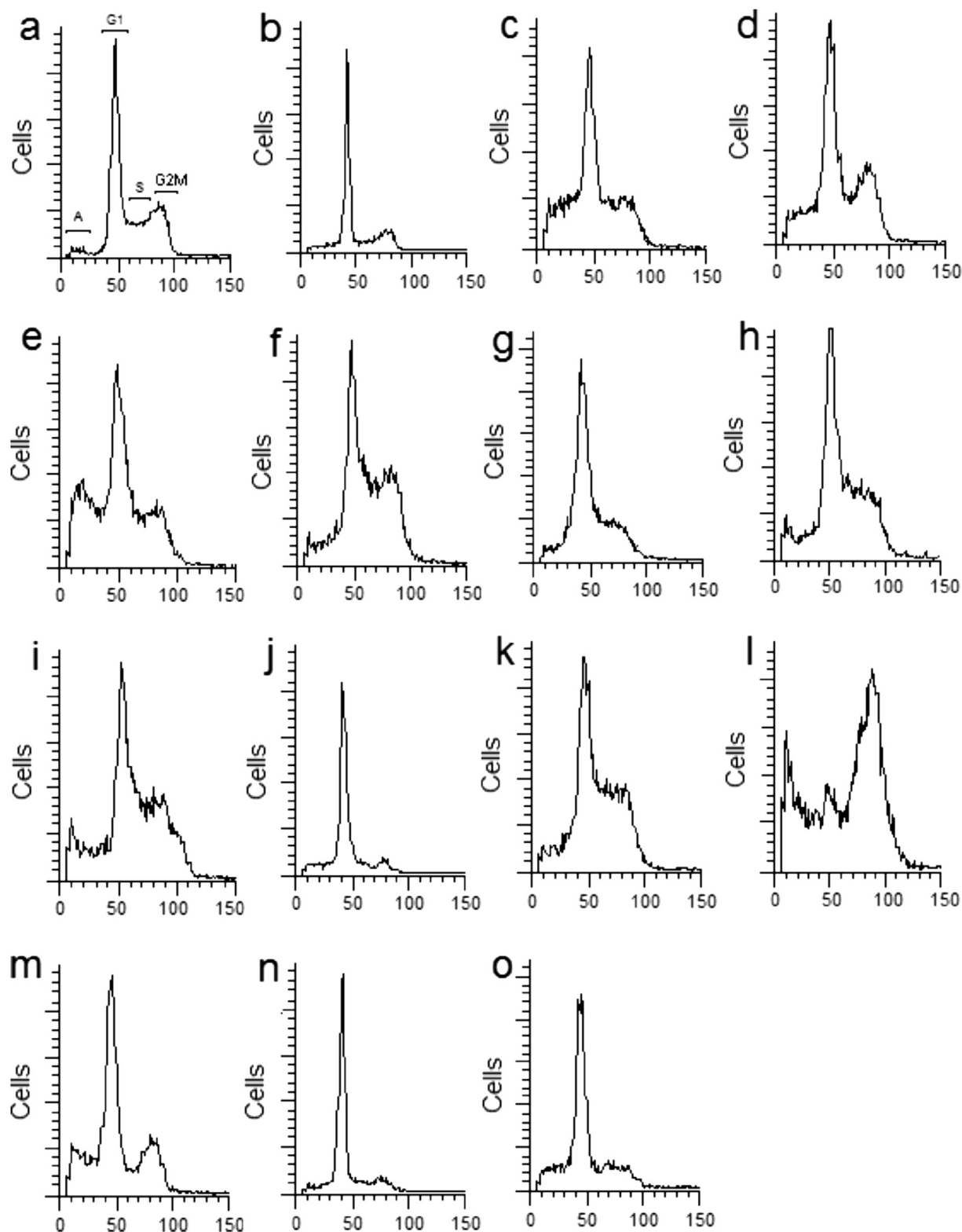


Fig. 1. Effects of compounds **4–9**, **11**, **13**, **15**, **17–20** and **23** on DNA content per cell following exposure of K562 cells for 24 h. a) control; b) **4** (3 μ M); c) **5** (2 μ M); d) **6** (0.5 μ M); e) **7** (0.75 μ M); f) **8** (2 μ M); g) **9** (2 μ M); h) **11** (3 μ M); i) **13** (3 μ M); j) **15** (2 μ M); k) **17** (2 μ M); l) **18** (2 μ M); m) **19** (3 μ M); n) **20** (1 μ M); o) **23** (5 μ M).

was found to be the most active derivative in the *in vitro* tubulin polymerization assay (IC_{50} = 1.1 μ M), 2-fold more active than *N*-methylindole analog **15** and reference compound **1**. Compound **20** was also more potent than **1** and **15** as an inhibitor of colchicine

binding. The two benzo[*b*]furan derivatives **4** and **23** did not alter tubulin assembly at concentrations as high as 20 μ M, nor did they inhibit colchicine binding to tubulin. Thus, the order of inhibitory effects on tubulin polymerization was **20** > **1** = **15** >> **4** = **23**. This

Table 2
Cell cycle distribution (%) of K562 cells after exposure to compounds.

Compound	G1	S	G2M
Control	39.27	47.84	12.89
4	75.37	20.98	3.65
5	43.33	52.26	4.41
6	35.78	35.47	28.76
7	34.66	57.32	8.02
8	33.67	53.09	16.24
9	39.48	53.52	7.00
11	37.06	51.30	11.1
13	31.82	57.79	9.39
15	77.64	19.55	2.81
17	32.96	54.92	12.12
18	19.94	33.70	45.36
19	41.47	27.66	30.87
20	79.88	17.13	2.99
23	68.32	20.28	11.40

order of activity as inhibitors of tubulin assembly correlates well with their order of activity as STAT5 modulators. We thus identified tubulin as an alternative molecular target of compounds **15** and **20**, since they strongly inhibited tubulin assembly and the binding of colchicine to tubulin. Their activity was greater than, or comparable with, that of the reference compound **1**. It should be noted, however, that neither **15** nor **20** caused an increase of the proportion of cells in the G2M phase of the cell cycle, and this is generally a hallmark of well characterized antitubulin agents.

4. Discussion

STAT5 activation is correlated with functional effects on cell cycle progression and resistance to apoptosis through increased expression of cyclin D1 and Bcl-xl, respectively [11,12] and is essential for leukemic cell survival [13,15]. Moreover, many studies have shown that the constitutive STAT5 activation induced by the Bcr–Abl oncogene plays an important role in the pathogenesis of CML [11–13], as shown by evidence that murine STAT5-null bone marrow cells were inefficient in generating and maintaining a CML-like disease [16].

Previously, we described the cytotoxic activity in Bcr–Abl expressing cells of a new class of substituted 2-(3',4',5'-trimethoxybenzoyl)benzo[b]furan derivatives. The 2-(3',4',5'-trimethoxybenzoyl)-3-iodoacetylamino-6-methoxybenzo[b]furan derivative **1** showed somewhat greater antiproliferative activity than imatinib and had the ability to decrease intracellular levels of pSTAT5 [45]. With the aim to discover more potent compounds for inhibition of the phosphorylation-activation of STAT5, we designed a new series of 2-aryloxy benzoheterocyclic derivatives structurally related to compound **1** and examined them for their ability to decrease pSTAT5 levels in K562 cells. SAR analysis indicated that (i) the benzo[b]furan nucleus was not indispensable for STAT5 inhibitory activity, for it could be replaced by benzo[b]thiophene or *N*-methyl indole systems, (ii) the *ortho* relationship between the benzoyl and the iodoacetylamino moieties at the C-2 and C-3 positions, respectively, of the benzoheterocyclic nucleus was essential for the STAT5 activity, and (iii) replacing the 3',4',5'-trimethoxybenzoyl moiety at the 2-position of benzo[b]furan skeleton with a benzoyl group maintained STAT5 inhibitory activity.

Compound **6** was the most active of the series in terms of antiproliferative and apoptosis activity (IC₅₀ = 0.07 μM, AC₅₀ = 0.25 μM). Compared to imatinib mesilate (IC₅₀ = 0.22 μM, AC₅₀ = 0.68 μM) it was 3 times more active as antiproliferative agent and 2 times more potent as apoptotic agent. The apoptotic effect observed with compound **6** in K562 cells is of interest considering that the Bcr–Abl oncogene expressed in this cell line

confers resistance toward apoptosis induced by different agents. Although this compound seemed to act primarily as an antimetabolic agent by blocking cells in the G2M phase, it also reduced the intracellular pSTAT5 levels. Compounds **18** and **19** also induced an arrest of cells in the G2M phase and were able to reduce the expression of pSTAT5. In contrast compounds **5**, **7**, **8**, **9**, **11**, **13** and **17** increased the proportion of cells in the S phase, but these agents had little or no ability to modulate STAT5. Compounds **1**, **15** and **20** were the most active in modulating STAT5 (they caused a complete or potent inhibition of STAT5 phosphorylation), and they strongly inhibited tubulin polymerization. However, these compounds caused a substantial increase in the proportion of cells in the G1 phase but not in the G2M phase as usually observed with antitubulin agents. This could be caused by their ability to potently inhibit STAT5 activation, thus preventing the G1 to S phase transition. In fact, pSTAT5 modulates the expression of genes that are known to regulate growth and survival, such as cyclin D1, Bcl-xl, c-Myc, pim-1, and p21 [48,49]. In addition, several of the genes modulated by pSTAT5 are known to be associated with lymphoproliferative disorders. This includes nucleobindin, which is associated with non-Hodgkin's lymphoma [50] and MIP-1α, which is associated with multiple myeloma [51].

Compared to the reference compound **1**, derivative **20** was slightly less cytotoxic, but it was able to decrease intracellular pSTAT5 levels more potently than **1** and at a markedly lower concentration (1 μM vs 7.5 μM). Except for the two benzo[b]furan derivatives **4** and **23** that had good activity in decreasing pSTAT5 expression, but did not show antitubulin activity, our data suggest that there is a correlation between antitubulin activity and inhibition of STAT5 phosphorylation. This is supported by other studies that show that antimetabolic agents can modulate STAT5 activity. Previous observations have shown the presence of a relationship between STATs nuclear translocation and microtubules. Indeed, the prevention of microtubule and microfilament polymerization induced a partial inhibition of STAT5 nuclear translocation and STAT5 DNA binding activity [52]. Moreover, paclitaxel, a microtubule stabilizer, significantly decreased the nuclear translocation of STATs without affecting the cytosolic tyrosine phosphorylation of these transcription factors [53]. Lopez-Perez and Salazar have shown that stimulation of MCF7 cells with epidermal growth factor (EGF) promoted an increase in the phosphorylation of STAT5 at Tyr-694 [52]. In addition, EGF stimulated STAT5 nuclear translocation and an increase in STAT5 DNA binding activity. STAT5 phosphorylation at Tyr-694 was dependent on the integrity of the microtubule network, and it was independent of the integrity of the actin cytoskeleton. This demonstrated for the first time that microtubules play an important role in STAT5 activation. Recently, a new microtubule destabilizing agent able to reduce phosphorylation/activation of a member of the STAT family member was described [54]. These observations are consistent with our data that show a correlation between tubulin polymerization inhibition and STAT5 phosphorylation/activation.

5. Conclusions

Among the inhibitors of STAT5 protein, our previous work led to the identification of compound **1** as a potent STAT5 inhibitor. This agent contains the 2-(3',4',5'-trimethoxybenzoyl)-3-iodoacetamido-6-methoxybenzo[b]furan ring system. This finding prompted us to study this compound class in more detail by the preparation of a series of 2-(3',4',5'-trimethoxybenzoyl) benzoheterocyclic derivatives characterized by the presence of benzo[b]furan, benzo[b]thiophene, indole and *N*-methylindole ring systems and to determine which analogs were able to target STAT5 and disrupt STAT5 signaling. For most of the synthesized molecules, the

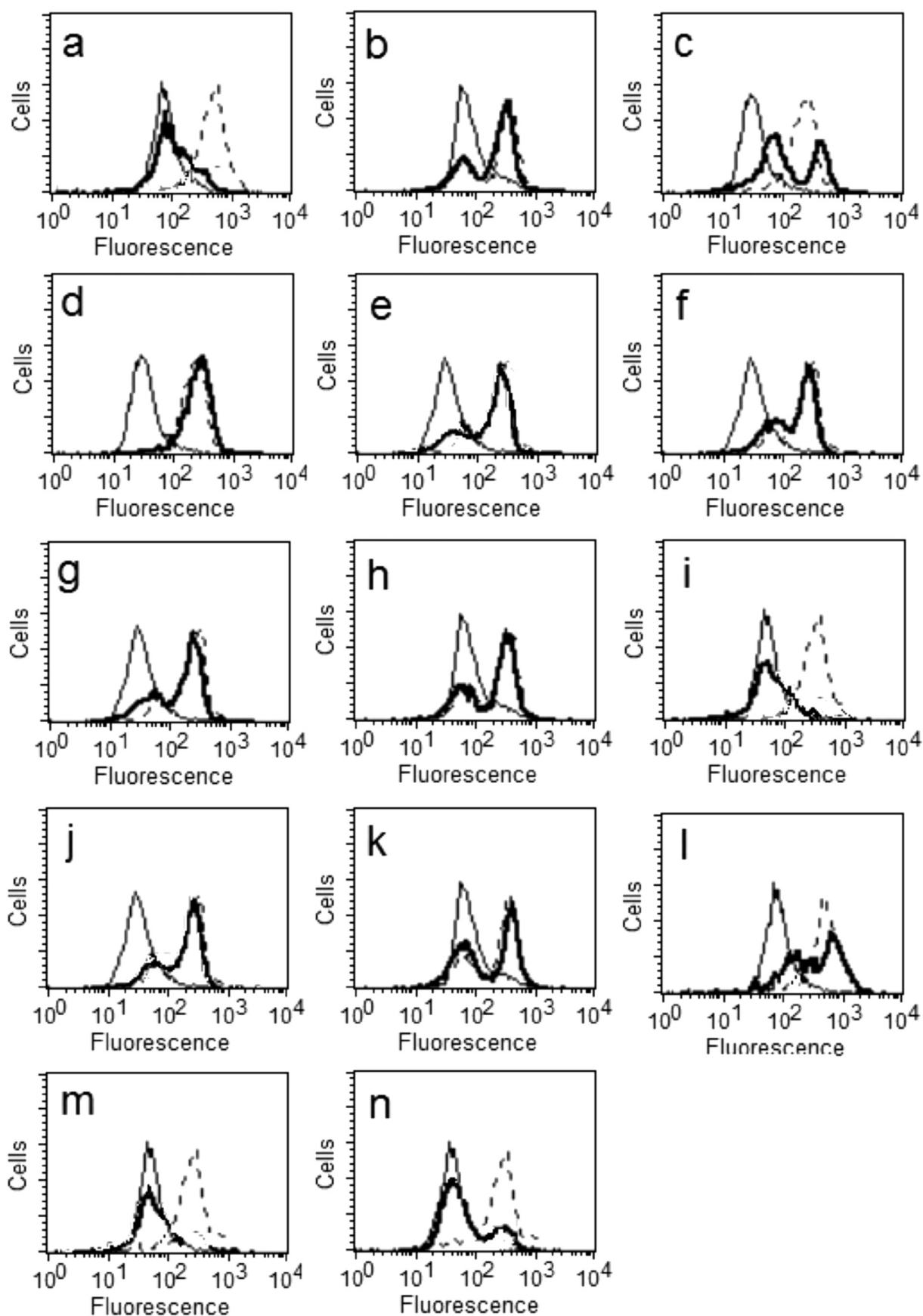


Fig. 2. Effects of compounds **4–9**, **11**, **13**, **15**, **17–20** and **23** on pSTAT5 expression in K562 cells. Intracellular levels of phosphorylated STAT5 were evaluated by flow cytometry after a 24 h exposure of cells to each compound as described in Materials and Methods. Thin line: cells stained with an isotype monoclonal antibody; dotted line: cells stained with an anti-pSTAT5 monoclonal antibody; thick line: cells stained with an anti-pSTAT5 monoclonal antibody after a 24 h exposure to each compound. a) **4** (3 μ M); b) **5** (2 μ M); c) **6** (0.5 μ M); d) **7** (0.75 μ M); e) **8** (2 μ M); f) **9** (2 μ M); g) **11** (3 μ M); h) **13** (3 μ M); i) **15** (2 μ M); j) **17** (2 μ M); k) **18** (2 μ M); l) **19** (3 μ M); m) **20** (1 μ M); n) **23** (5 μ M).

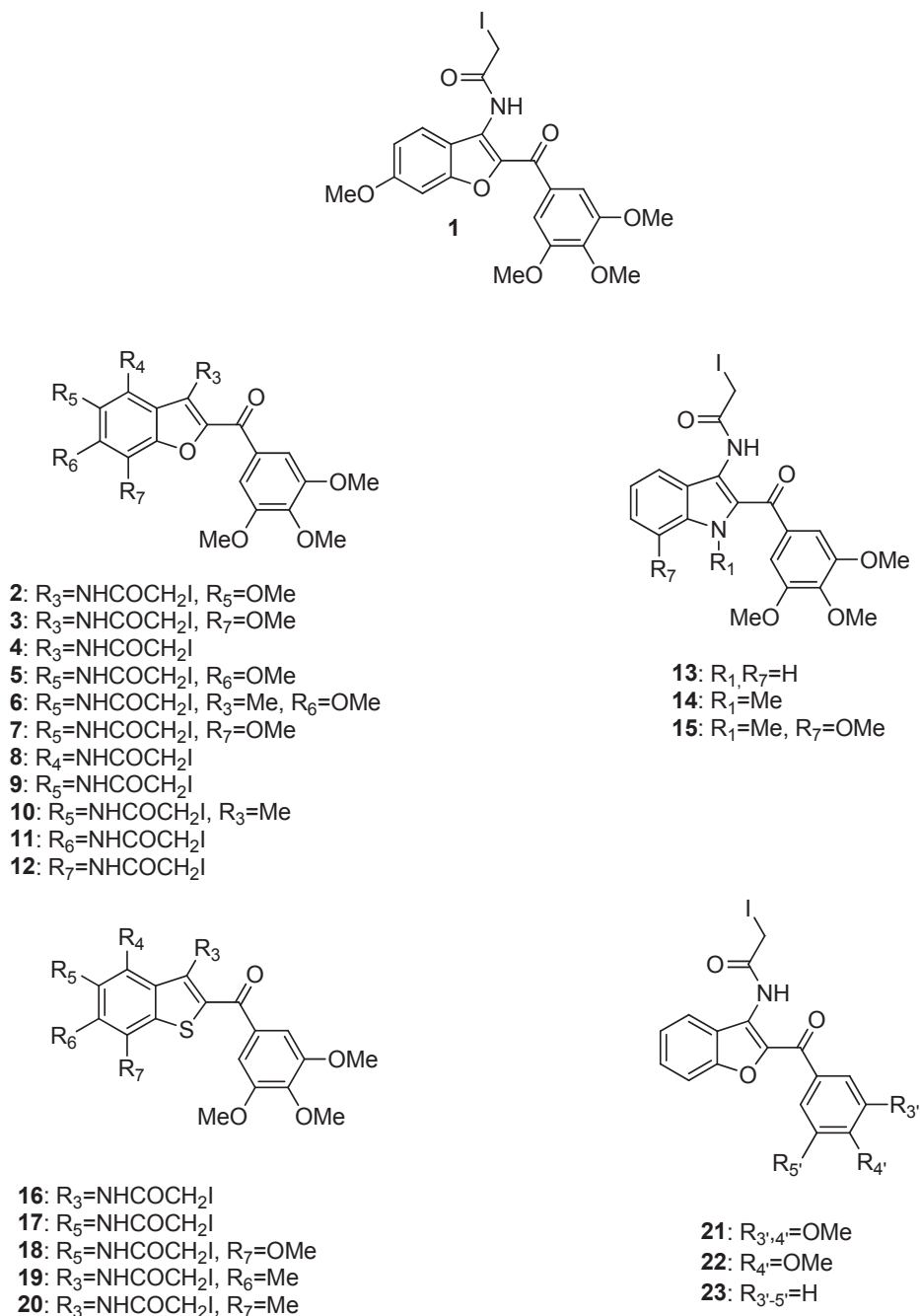


Chart 1. Structure of reference compound **1** and new iodoacetamido 2-aryl benzoheterocyclic derivatives **2–23** ($R = \text{H}$, if not specified).

3',4',5'-trimethoxybenzoyl substituent was maintained at the 2-position of the benzoheterocycle, and we examined the effect on biological activity by altering the positions of the iodoacetamido group and of methyl and methoxy moieties, moving these substituents from the C-3 to C-7 positions. The SAR study indicated that the presence of the methoxy group located at the C-6 position of the benzo[*b*]furan nucleus contributed to maximal activity, since the C-5 and C-7 methoxy analogs **2** and **3**, respectively, were considerably less active than the C-6 methoxy counterpart **1**. In the series of 5-iodoacetamido benzo[*b*]furan derivatives **5–7** and **10**, the greatest antiproliferative activity occurred with the concomitant presence of a methyl and methoxy group at the C-3 and C-6 positions, respectively, the least when a single methyl group was

inserted at the C-3 position, to yield compounds **6** and **10**, respectively, while the C-6 and C-7 methoxy analogs **5** and **7** were equipotent. The most active compound identified in this study was the 2-(3',4',5'-trimethoxybenzoyl)-3-methyl-5-(iodoacetylamino)-6-methoxybenzo[*b*]furan derivative **6**, which was twice as active as **1** with K562 cells.

A moderate increase of activity was observed moving the iodoacetamido group from the C-3 to the C-4 position of the benzo[*b*]furan ring, while only a marginal improvement occurred by shifting the iodoacetamido function from the C-4 to the C-5 or C-6 positions (compounds **4**, **8**, **9** and **11**, respectively). Compound **12**, with the iodoacetylamino moiety at the C-7 position, had no antiproliferative activity ($\text{IC}_{50} > 50 \mu\text{M}$). In the series of 3-

Table 3

Median fluorescence values of K562 cells stained with an anti-pSTAT5 antibody after 24 h exposure to compounds.

Compounds	Median fluorescence
Control (Isotypic MoAb)	44.54
Control (pSTAT5 MoAb)	315.56
1	54.33
4	98.34
5	224.76
6	176.07
7	316.21
8	271.63
9	254.88
11	288.76
13	221.92
15	58.23
17	278.54
18	201.32
19	199.87
20	45.22
23	103.25

Control (Isotypic MoAb) = K562 cells stained with an isotypic MoAb.

Control (STAT5 MoAb) = K562 cells stained with a STAT5 MoAb.

Compound **1** was used at 7.5 μ M.

Table 4

Inhibition of tubulin polymerization and colchicine binding by compounds **1**, **4**, **15**, **20** and **23**.

Compound	Tubulin assembly ^a IC ₅₀ \pm SD (μ M)	Colchicine binding ^b % \pm SD
4	>20	N.d.
15	2.0 \pm 0.3	38 \pm 0.0
20	1.1 \pm 0.06	65 \pm 4
23	>20	N.d.
1	1.8 \pm 0.1	54 \pm 1

^a Inhibition of tubulin polymerization. Tubulin was at 10 μ M.

^b Inhibition of [³H]colchicine binding. Tubulin, colchicine and tested compound were at 1, 5 and 5 μ M, respectively. N.d.: not determined.

iodoacetamido benzoheterocyclic derivatives **4**, **13**, **14** and **16**, the antiproliferative activity of benzo[*b*]furan derivative **4** was 15-fold greater than that of benzo[*b*]thiophene counterpart **16**, 2-fold lower than that of indole derivative **13** and 4-fold higher than that of *N*-methylindole **14**. The marked improvement in activity of compounds **19** and **20** related to 2-(3',4',5'-trimethoxybenzoyl)-3-iodoacetyl amino benzo[*b*]thiophene derivative **16** derives from the introduction of a methyl group at the C-6 or C-7 positions of the benzo[*b*]thiophene core, respectively. Among the two isomeric methyl benzo[*b*]thiophene derivatives, simply moving the methyl group from the C-6 to the C-7 position, to furnish derivative **19** and **20**, respectively, a two-fold improvement of activity occurred.

Four compounds of this series (**4**, **15**, **20** and **23**) with substantially greater antiproliferative activity than **1** had significant inhibitory activities on STAT5 activation. These compounds, like reference compound **1**, blocked cells in G1.

As with reference compound **1**, derivatives **15** and **20** were able both to decrease the pSTAT5 level and to inhibit the assembly of tubulin by interacting with tubulin at the colchicine site. For the two benzo[*b*]furan derivatives **4** and **23**, which were less active in modulating STAT5 than **1**, **15** and **20**, it was possible to achieve a complete separation between these two effects, since compounds **4** and **23** had minimal antitubulin activity. The ability of 2-benzoyl-3-iodoacetamidobenzo[*b*]furan derivative **23** to reduce markedly the expression of activated STAT5 demonstrated that the presence of the three methoxy groups on the 2-benzoyl moiety was not essential for anti-STAT5 activity.

We have no specific evidence that our compounds alkylate

intracellular proteins, thereby interfering with STAT activation, and we feel this possibility is too speculative to discuss at this time. The mechanism by which the new molecules **4**, **15**, **20** and **23** modulates STAT5 expression remains to be elucidated and is currently under investigation.

6. Experimental section

6.1. Chemistry

6.1.1. Materials and methods

¹H NMR and ¹³C NMR spectra were determined in CDCl₃ or *d*₆-DMSO solutions and recorded with a Varian VXR-200 spectrometer or a Varian Mercury Plus 400 spectrometer. Chemical shifts (δ) are given in parts per million (ppm) downfield and J values are given in hertz. Positive-ion electrospray ionization (ESI) mass spectra were recorded on a double-focusing ESI Micromass ZMD 2000 mass spectrometer. Melting points (mp) were determined on a Buchi–Tottoli apparatus and are uncorrected. Elemental analyses were conducted by the Microanalytical Laboratory of the Chemistry Department of the University of Ferrara and were performed on a Yanagimoto MT-5 CHN recorder analyzer. All tested compounds yielded data consistent with a purity of at least 95% as compared with the theoretical values. Reaction courses and product mixtures were routinely monitored by TLC on silica gel (precoated F₂₅₄ Merck plates) and visualized with aqueous KMnO₄. Flash chromatography was performed using 230–400 mesh silica gel and the solvent system indicated in the procedure. All commercially available compounds were used without further purification. Organic solutions were dried over anhydrous Na₂SO₄. Petroleum ether refers to the fraction boiling at 40–60 °C.

6.1.2. General procedure A for the preparation of compounds 38–51

To a solution of aminobenzoheterocyclic derivative **24–37** (1 mmol) and pyridine (3 mmol, 0.24 mL) in dry CH₂Cl₂ (5 mL), bromoacetyl bromide (0.25 mL, 3 mmol) was added at 0 °C. After 1 h at the same temperature, the reaction mixture was diluted with CH₂Cl₂ (5 mL), washed with water (5 mL), dried over Na₂SO₄ and concentrated *in vacuo*. The crude residue was purified by flash chromatography on silica gel.

6.1.2.1. 2-Bromo-*N*-(6-methoxy-2-(3,4,5-trimethoxybenzoyl)benzofuran-5-yl)acetamide (**38**). Following general procedure A, the crude residue purified by flash chromatography using ethyl acetate: petroleum ether 1:1 (v:v) as eluent furnished **38** as a white solid. Yield: 83%; mp 185–187 °C. ¹H NMR (CDCl₃) δ : 3.94 (s, 6H), 3.96 (s, 3H), 4.03 (s, 3H), 4.07 (s, 2H), 7.15 (s, 1H), 7.27 (s, 2H), 7.48 (s, 1H), 8.69 (s, 1H), 8.82 (bs, 1H). MS (ESI): [M+1]⁺ = 478.1 and 480.1.

6.1.2.2. 2-Bromo-*N*-(6-methoxy-3-methyl-2-(3,4,5-trimethoxybenzoyl)benzofuran-5-yl)acetamide (**39**). Following general procedure A, the crude residue purified by flash chromatography using ethyl acetate: petroleum ether 1:1 (v:v) as eluent furnished **39** as a yellow solid. Yield: 81%; mp 128–130 °C. ¹H NMR (CDCl₃) δ : 2.60 (s, 3H), 3.93 (s, 3H), 3.95 (s, 6H), 4.01 (s, 3H), 4.08 (s, 2H), 7.04 (s, 1H), 7.36 (s, 2H), 8.65 (s, 1H), 8.86 (bs, 1H). MS (ESI): [M+1]⁺ = 491.1 and 493.2.

6.1.2.3. 2-Bromo-*N*-[7-methoxy-2-(3,4,5-trimethoxybenzoyl)-1-benzofuran-5-yl]acetamide (**40**). Following general procedure A, the crude residue purified by flash chromatography using ethyl acetate: petroleum ether 4:6 (v:v) as eluent furnished **40** as a cream colored solid. Yield: 68%; mp 192–194 °C. ¹H NMR (CDCl₃) δ : 3.95 (s, 3H), 3.96 (s, 6H), 4.04 (s, 3H), 4.07 (s, 2H), 7.17 (s, 1H), 7.28 (s, 2H), 7.42 (s, 1H), 7.53 (s, 1H), 8.22 (bs, 1H). MS (ESI): [M+1]⁺ = 478.3 and

480.3.

6.1.2.4. *2-Bromo-N-(2-(3,4,5-trimethoxybenzoyl)benzofuran-4-yl)acetamide (41)*. Following general procedure A, the crude residue purified by flash chromatography using ethyl acetate: petroleum ether 1:1 (v:v) as eluent furnished **41** as a yellow solid. Yield: 74%; mp 163–164 °C. $^1\text{H NMR}$ (CDCl_3) δ : 3.95 (s, 3H), 3.97 (s, 6H), 4.11 (s, 2H), 7.37 (s, 2H), 7.48 (m, 2H), 7.59 (s, 1H), 7.74 (m, 1H), 8.53 (bs, 1H). MS (ESI): $[\text{M}+1]^+ = 448.5$ and 450.5.

6.1.2.5. *2-Bromo-N-[2-(3,4,5-trimethoxybenzoyl)-1-benzofuran-5-yl]acetamide (42)*. Following general procedure A, the crude residue purified by flash chromatography using ethyl acetate: petroleum ether 4:6 (v:v) as eluent furnished **42** as a brown solid. Yield: 78%; mp 68–70 °C. $^1\text{H NMR}$ (CDCl_3) δ : 3.94 (s, 3H), 3.96 (s, 6H), 4.11 (s, 2H), 7.34 (s, 2H), 7.42 (dd, $J = 8.0$ and 2.0 Hz, 1H), 7.52 (s, 1H), 7.59 (d, $J = 8.0$ Hz, 1H), 8.18 (d, $J = 2.0$ Hz, 1H), 8.32 (bs, 1H). MS (ESI): $[\text{M}+1]^+ = 448.4$ and 450.4.

6.1.2.6. *2-Bromo-N-(3-methyl-2-(3,4,5-trimethoxybenzoyl)benzofuran-5-yl)acetamide (43)*. Following general procedure A, the crude residue purified by flash chromatography using ethyl acetate: petroleum ether 1:1 (v:v) as eluent furnished **43** as a pink solid. Yield: 79%; mp 174–176 °C. $^1\text{H NMR}$ (CDCl_3) δ : 2.62 (s, 3H), 3.93 (s, 6H), 3.96 (s, 3H), 4.08 (s, 2H), 7.39 (s, 2H), 7.49 (m, 2H), 8.04 (s, 1H), 8.23 (bs, 1H). MS (ESI): $[\text{M}+1]^+ = 462.4$ and 464.4.

6.1.2.7. *2-Bromo-N-(2-(3,4,5-trimethoxybenzoyl)benzofuran-6-yl)acetamide (44)*. Following general procedure A, the crude residue purified by flash chromatography using ethyl acetate: petroleum ether 1:1 (v:v) as eluent furnished **44** as a pink solid. Yield: 84%; mp 174–176 °C. $^1\text{H NMR}$ (d_6 -DMSO) δ : 3.78 (s, 2H), 3.88 (s, 6H), 4.10 (s, 3H), 7.27 (s, 2H), 7.48 (dd, $J = 8.6$ and 1.8 Hz, 1H), 7.78 (d, $J = 8.6$ Hz, 1H), 7.85 (s, 1H), 8.18 (s, 1H), 10.8 (bs, 1H). MS (ESI): $[\text{M}+1]^+ = 448.4$ and 450.4.

6.1.2.8. *2-Bromo-N-(2-(3,4,5-trimethoxybenzoyl)benzofuran-7-yl)acetamide (45)*. Following general procedure A, the crude residue purified by flash chromatography using ethyl acetate: petroleum ether 1:1 (v:v) as eluent furnished **45** as a purple solid. Yield: 77%; mp 156–168 °C. $^1\text{H NMR}$ (d_6 -DMSO) δ : 3.80 (s, 2H), 3.88 (s, 6H), 3.91 (s, 3H), 7.30 (s, 2H), 7.63 (d, $J = 8.4$ Hz, 1H), 7.96 (s, 1H), 8.72 (t, $J = 8.4$ Hz, 1H), 9.13 (d, $J = 8.4$ Hz, 1H), 11.3 (bs, 1H). MS (ESI): $[\text{M}+1]^+ = 448.6$ and 450.7.

6.1.2.9. *2-Bromo-N-(2-(3,4,5-trimethoxybenzoyl)-1H-indol-3-yl)acetamide (46)*. Following general procedure A, the crude residue purified by flash chromatography using ethyl acetate: petroleum ether 4:6 (v:v) as eluent furnished **46** as a brown solid. Yield: 77%; mp 208–210 °C. $^1\text{H NMR}$ (CDCl_3) δ : 3.89 (s, 6H), 3.93 (s, 3H), 4.06 (s, 2H), 7.07 (s, 2H), 7.21 (m, 2H), 7.37 (m, 1H), 8.10 (d, $J = 8.4$ Hz, 1H), 8.62 (bs, 1H), 10.3 (bs, 1H). MS (ESI): $[\text{M}+1]^+ = 447.3$ and 449.3.

6.1.2.10. *2-Bromo-N-(1-methyl-2-(3,4,5-trimethoxybenzoyl)-1H-indol-3-yl)acetamide (47)*. Following general procedure A, the crude residue purified by flash chromatography using ethyl acetate: petroleum ether 1:1 (v:v) as eluent furnished **47** as a brown solid. Yield: 87%; mp 216–217 °C. $^1\text{H NMR}$ (CDCl_3) δ : 1.57 (s, 3H), 3.79 (s, 2H), 3.87 (s, 3H), 3.89 (s, 3H), 3.94 (s, 3H), 7.09 (s, 2H), 7.21 (m, 2H), 7.41 (m, 1H), 7.70 (d, $J = 8.2$ Hz, 1H), 8.63 (bs, 1H). MS (ESI): $[\text{M}+1]^+ = 461.4$ and 463.4.

6.1.2.11. *2-Bromo-N-(7-methoxy-1-methyl-2-(3,4,5-trimethoxybenzoyl)-1H-indol-3-yl)acetamide (48)*. Following general procedure A, the crude residue purified by flash

chromatography using ethyl acetate: petroleum ether 4:6 (v:v) as eluent furnished **48** as a brown solid. Yield: 83%; mp 178–180 °C. $^1\text{H NMR}$ (CDCl_3) δ : 3.87 (s, 3H), 3.92 (s, 6H), 3.94 (s, 3H), 3.98 (s, 3H), 4.03 (s, 2H), 6.77 (d, $J = 7.6$ Hz, 1H), 7.07 (m, 1H), 7.11 (s, 2H), 7.21 (d, $J = 7.6$ Hz, 1H), 8.72 (bs, 1H). MS (ESI): $[\text{M}+1]^+ = 491.1$ and 493.1.

6.1.2.12. *2-Bromo-N-(2-(3,4-dimethoxybenzoyl)benzofuran-3-yl)acetamide (49)*. Following general procedure A, the crude residue purified by flash chromatography using ethyl acetate: petroleum ether 1:1 (v:v) as eluent furnished **49** as a brown solid. Yield: 83%; mp 138–140 °C. $^1\text{H NMR}$ (CDCl_3) δ : 3.98 (s, 3H), 4.00 (s, 3H), 4.14 (s, 2H), 7.04 (d, $J = 8.6$ Hz, 1H), 7.33 (m, 2H), 7.52 (dd, $J = 5.4$ and 2.0 Hz, 1H), 7.78 (d, $J = 2.0$ Hz, 1H), 8.13 (dd, $J = 8.0$ and 1.8 Hz, 1H), 8.48 (d, $J = 8.0$ Hz, 1H), 11.4 (bs, 1H). MS (ESI): $[\text{M}+1]^+ = 418.4$ and 420.4.

6.1.2.13. *2-Bromo-N-(2-(4-methoxybenzoyl)benzofuran-3-yl)acetamide (50)*. Following general procedure A, the crude residue purified by flash chromatography using ethyl acetate: petroleum ether 4:6 (v:v) as eluent furnished **50** as a cream colored solid. Yield: 95%; mp 140–142 °C. $^1\text{H NMR}$ (CDCl_3) δ : 3.92 (s, 3H), 4.13 (s, 2H), 7.07 (m, 2H), 7.33 (m, 2H), 7.54 (dd, $J = 6.8$ and 2.0 Hz, 1H), 8.31 (dd, $J = 6.8$ and 1.6 Hz, 2H), 8.47 (dd, $J = 8.0$ and 1.6 Hz, 1H), 11.5 (bs, 1H). MS (ESI): $[\text{M}+1]^+ = 388.4$ and 390.4.

6.1.2.14. *N-(2-Benzoylbenzofuran-3-yl)-2-bromoacetamide (51)*. Following general procedure A, the crude residue purified by flash chromatography using ethyl acetate: petroleum ether 2:8 (v:v) as eluent furnished **51** as a yellow solid. Yield: 76%; mp 87–88 °C. $^1\text{H NMR}$ (CDCl_3) δ : 4.15 (s, 2H), 7.34 (m, 1H), 7.53 (m, 2H), 7.63 (m, 3H), 8.22 (dd, $J = 8.4$ and 1.6 Hz, 2H), 8.50 (d, $J = 8.4$ Hz, 1H), 11.4 (bs, 1H). MS (ESI): $[\text{M}+1]^+ = 358.1$ and 360.1.

6.1.3. General procedure B for the synthesis of compounds 5–15 and 21–23

A mixture of bromoacetamido derivatives **38–51** (1 mmol) and NaI (1.5 g, 10 mmol) in *N,N*-dimethylacetamide (5 mL) was stirred at ambient temperature for 18 h. *N,N*-dimethylacetamide was evaporated under reduced pressure, followed by addition of CH_2Cl_2 (15 mL) and a solution of $\text{Na}_2\text{S}_2\text{O}_3$ (10%, 5 mL). The organic layer was washed with water (5 mL) and brine (5 mL) and dried over Na_2SO_4 . After evaporation of the solvent, the residue was purified by flash chromatography on silica gel.

6.1.3.1. *2-Iodo-N-(6-methoxy-2-(3,4,5-trimethoxybenzoyl)benzofuran-5-yl)acetamide (5)*. Following general procedure B, the crude residue purified by flash chromatography using ethyl acetate: petroleum ether 1:1 (v:v) as eluent furnished **5** as a yellow solid. Yield: 73%; mp 192–194 °C. $^1\text{H NMR}$ (CDCl_3) δ : 3.92 (s, 2H), 3.94 (s, 6H), 3.96 (s, 3H), 4.03 (s, 3H), 7.13 (s, 1H), 7.27 (s, 2H), 7.47 (s, 1H), 8.38 (bs, 1H), 8.68 (bs, 1H). $^{13}\text{C NMR}$ (CDCl_3) δ : 0.145, 56.48 (2C), 56.60, 61.13, 94.39, 106.99 (2C), 112.94 (2C), 117.47, 119.88, 125.35, 132.56, 142.42, 150.47, 152.07, 153.18, 153.45, 164.99, 182.73. MS (ESI): $[\text{M}+1]^+ = 526.6$. Anal. calcd for $\text{C}_{21}\text{H}_{20}\text{INO}_7$ C, 48.02; H, 3.84; N, 2.67; found: C, 47.88; H, 3.69; N, 2.59.

6.1.3.2. *2-Iodo-N-(6-methoxy-3-methyl-2-(3,4,5-trimethoxybenzoyl)benzofuran-5-yl)acetamide (6)*. Following general procedure B, the crude residue purified by flash chromatography using ethyl acetate: petroleum ether 1:1 (v:v) as eluent furnished **6** as a yellow solid. Yield: 81%; mp 172–174 °C. $^1\text{H NMR}$ (CDCl_3) δ : 2.59 (s, 3H), 3.93 (s, 8H), 3.95 (s, 3H), 4.00 (s, 3H), 7.02 (s, 1H), 7.35 (s, 2H), 8.38 (s, 1H), 8.63 (bs, 1H). $^{13}\text{C NMR}$ (CDCl_3) δ : 0.26, 10.48, 56.41 (2C), 56.54, 61.07, 94.04, 107.36 (2C), 111.37 (2C), 122.13, 124.84, 128.22, 133.17, 142.11, 148.46, 150.41, 151.49, 152.92, 164.90, 184.01. MS (ESI): $[\text{M}+1]^+ = 540.3$. Anal. calcd for $\text{C}_{22}\text{H}_{22}\text{INO}_7$ C, 48.99; H, 4.11; N,

2.60; found: C, 48.78; H, 3.89; N, 2.48.

6.1.3.3. 2-Iodo-N-[7-methoxy-2-(3,4,5-trimethoxybenzoyl)-1-benzofuran-5-yl]acetamide (7). Following general procedure B, the crude residue purified by flash chromatography using ethyl acetate: petroleum ether 1:1 (v:v) as eluent furnished **7** as a yellow solid. Yield: 71%; mp 190–191 °C. ¹H NMR (*d*₆-DMSO) δ: 3.79 (s, 3H), 3.85 (s, 2H), 3.88 (s, 6H), 3.97 (s, 3H), 7.22 (d, *J* = 1.6 Hz, 1H), 7.29 (s, 2H), 7.80 (d, *J* = 1.6 Hz, 1H), 7.88 (s, 1H), 10.5 (bs, 1H). ¹³C NMR (*d*₆-DMSO) δ: 1.44, 55.96 (2C), 60.12 (2C), 102.94, 104.45, 106.72 (2C), 117.38 (2C), 128.20, 131.67, 135.82, 141.52, 141.66, 144.96, 151.64, 152.65, 166.54, 181.97. MS (ESI): [M+1]⁺ = 526.6. Anal. calcd for C₂₁H₂₀INO₇ C, 48.02; H, 3.84; N, 2.67; found: C, 47.91; H, 3.70; N, 2.49.

6.1.3.4. 2-Iodo-N-(2-(3,4,5-trimethoxybenzoyl)benzofuran-4-yl)acetamide (8). Following general procedure B, the crude residue purified by flash chromatography using ethyl acetate: petroleum ether 4:6 (v:v) as eluent furnished **8** as a green solid. Yield: 78%; mp 167–168 °C. ¹H NMR (CDCl₃) δ: 3.95 (s, 8H), 3.97 (s, 3H), 7.35 (s, 2H), 7.43 (m, 2H), 7.60 (m, 1H), 7.64 (s, 1H), 8.12 (bs, 1H). ¹³C NMR (CDCl₃) δ: -0.53, 56.39 (2C), 61.07, 107.17 (2C), 109.69, 114.24, 115.98 (2C), 120.42, 128.86, 131.68, 131.81, 142.59, 151.48, 153.04, 156.31, 165.51, 182.96. MS (ESI): [M+1]⁺ = 496.6. Anal. calcd for C₂₀H₁₈INO₆ C, 48.50; H, 3.66; N, 2.83; found: C, 48.29; H, 3.51; N, 2.62.

6.1.3.5. 2-Iodo-N-[2-(3,4,5-trimethoxybenzoyl)-1-benzofuran-5-yl]acetamide (9). Following general procedure B, the crude residue purified by flash chromatography using ethyl acetate: petroleum ether 1:1 (v:v) as eluent furnished **9** as a brown solid. Yield: 68%; mp 185–187 °C. ¹H NMR (*d*₆-DMSO) δ: 3.79 (s, 3H), 3.86 (s, 2H), 3.89 (s, 6H), 7.29 (s, 2H), 7.53 (dd, *J* = 9.2 and 2.0 Hz, 1H), 7.73 (d, *J* = 9.2 Hz, 1H), 7.91 (s, 1H), 8.27 (d, *J* = 2.0 Hz, 1H), 10.5 (bs, 1H). ¹³C NMR (*d*₆-DMSO) δ: 1.41, 55.98 (2C), 60.12, 106.68 (2C), 112.41 (2C), 112.97 (2C), 117.30, 120.99, 127.08, 131.74, 135.11, 141.63, 151.72, 152.67, 166.57, 182.18. MS (ESI): [M+1]⁺ = 496.5. Anal. calcd for C₂₀H₁₈INO₆ C, 48.50; H, 3.66; N, 2.83; found: C, 48.31; H, 3.47; N, 2.63.

6.1.3.6. 2-Iodo-N-(3-methyl-2-(3,4,5-trimethoxybenzoyl)benzofuran-5-yl)acetamide (10). Following general procedure B, the crude residue purified by flash chromatography using ethyl acetate: petroleum ether 1:1 (v:v) as eluent furnished **10** as a pink solid. Yield: 80%; mp 173–175 °C. ¹H NMR (*d*₆-DMSO) δ: 2.52 (s, 3H), 3.79 (s, 3H), 3.86 (s, 6H), 3.88 (s, 2H), 7.33 (s, 2H), 7.55 (dd, *J* = 8.8 and 2.0 Hz, 1H), 7.69 (d, *J* = 8.8 Hz, 1H), 8.17 (d, *J* = 2.0 Hz, 1H), 10.5 (bs, 1H). ¹³C NMR (*d*₆-DMSO) δ: 1.54, 9.82, 56.06 (2C), 60.23, 107.07 (2C), 110.83, 112.60, 121.20 (2C), 125.99, 128.68, 132.36, 134.98, 141.65, 148.22, 150.20, 152.61, 166.62, 183.77. MS (ESI): [M+1]⁺ = 510.7. Anal. calcd for C₂₁H₂₀INO₆ C, 49.52; H, 3.96; N, 2.75; found: C, 49.37; H, 3.78; N, 2.61.

6.1.3.7. 2-Iodo-N-(2-(3,4,5-trimethoxybenzoyl)benzofuran-6-yl)acetamide (11). Following general procedure B, the crude residue purified by flash chromatography using ethyl acetate: petroleum ether 1:1 (v:v) as eluent furnished **11** as a yellow solid. Yield: 81%; mp 188–190 °C. ¹H NMR (*d*₆-DMSO) δ: 3.78 (s, 3H), 3.88 (s, 8H), 7.27 (s, 2H), 7.42 (dd, *J* = 8.4 and 1.6 Hz, 1H), 7.78 (d, *J* = 8.4 Hz, 1H), 7.84 (s, 1H), 8.17 (s, 1H), 10.7 (bs, 1H). ¹³C NMR (*d*₆-DMSO) δ: 1.31, 55.98 (2C), 60.09, 101.52, 106.58 (2C), 116.38, 117.36, 122.54, 124.06 (2C), 131.94, 139.55, 141.50, 151.28, 152.65, 155.68, 166.95, 181.83. MS (ESI): [M+1]⁺ = 496.7. Anal. calcd for C₂₀H₁₈INO₆ C, 48.50; H, 3.66; N, 2.83; found: C, 48.27; H, 3.48; N, 2.59.

6.1.3.8. 2-Iodo-N-(2-(3,4,5-trimethoxybenzoyl)benzofuran-7-yl)acetamide (12). Following general procedure B, the crude residue purified by flash chromatography using ethyl acetate: petroleum ether 1:1 (v:v) as eluent furnished **12** as a white solid. Yield: 78%; mp 193–195 °C. ¹H NMR (*d*₆-DMSO) δ: 3.81 (s, 2H), 3.89 (s, 6H), 3.93 (s, 3H), 7.32 (s, 2H), 7.66 (d, *J* = 8.4 Hz, 1H), 7.96 (s, 1H), 8.76 (t, *J* = 8.4 Hz, 1H), 9.09 (d, *J* = 8.4 Hz, 1H), 11.2 (bs, 1H). ¹³C NMR (CDCl₃) δ: 1.49, 55.91 (2C), 56.02, 102.25, 103.22, 107.06 (2C), 126.21, 129.76, 130.01, 132.13, 135.66, 139.75, 141.56, 145.07, 148.01, 152.48, 166.51, 183.34. MS (ESI): [M+1]⁺ = 496.1. Anal. calcd for C₂₀H₁₈INO₆ C, 48.50; H, 3.66; N, 2.83; found: C, 48.30; H, 3.51; N, 2.63.

6.1.3.9. 2-Iodo-N-(2-(3,4,5-trimethoxybenzoyl)-1H-indol-3-yl)acetamide (13). Following general procedure B, the crude residue purified by flash chromatography using ethyl acetate: petroleum ether 4:6 (v:v) as eluent furnished **13** as a cream colored solid. Yield: 83%; mp 215–217 °C. ¹H NMR (CDCl₃) δ: 3.90 (s, 6H), 3.93 (s, 5H), 7.05 (s, 2H), 7.16 (t, *J* = 8.4 Hz, 1H), 7.38 (m, 2H), 8.13 (d, *J* = 8.4 Hz, 1H), 8.61 (bs, 1H), 10.1 (bs, 1H). ¹³C NMR (CDCl₃) δ: -1.04, 56.46 (2C), 61.11, 106.10 (2C), 112.00, 121.13 (2C), 120.96, 121.07, 122.55, 124.94, 125.05, 127.66, 133.23, 136.26, 153.44, 165.71, 187.34. MS (ESI): [M+1]⁺ = 495.3. Anal. calcd for C₂₀H₁₉IN₂O₅ C, 48.60; H, 3.87; N, 5.63; found: C, 48.34; H, 3.67; N, 5.38.

6.1.3.10. 2-Iodo-N-(1-methyl-2-(3,4,5-trimethoxybenzoyl)-1H-indol-3-yl)acetamide (14). Following general procedure B, the crude residue purified by flash chromatography using ethyl acetate: petroleum ether 4:6 (v:v) as eluent furnished **14** as a yellow solid. Yield: 79%; mp 239–241 °C. ¹H NMR (*d*₆-DMSO) δ: 3.58 (s, 2H), 3.74 (s, 3H), 3.79 (s, 6H), 3.81 (s, 3H), 7.07 (s, 2H), 7.16 (t, *J* = 8.0 Hz, 1H), 7.37 (t, *J* = 8.0 Hz, 1H), 7.55 (d, *J* = 8.0 Hz, 1H), 7.61 (d, *J* = 8.0 Hz, 1H), 10.0 (bs, 1H). ¹³C NMR (*d*₆-DMSO) δ: 0.112, 31.69, 56.22 (2C), 60.64, 107.25 (2C), 111.28, 116.93, 120.58 (2C), 122.28, 125.40, 128.82, 133.96, 133.78, 137.37, 142.38, 153.13, 166.95, 187.05. MS (ESI): [M+1]⁺ = 509.7. Anal. calcd for C₂₁H₂₁IN₂O₅ C, 48.60; H, 3.87; N, 5.67; found: C, 48.29; H, 3.59; N, 5.40.

6.1.3.11. 2-Iodo-N-(7-methoxy-1-methyl-2-(3,4,5-trimethoxybenzoyl)-1H-indol-3-yl)acetamide (15). Following general procedure B, the crude residue purified by flash chromatography using ethyl acetate: petroleum ether 1:1 (v:v) as eluent furnished **15** as a yellow solid. Yield: 81%; mp 245–247 °C. ¹H NMR (*d*₆-DMSO) δ: 3.56 (s, 2H), 3.73 (s, 3H), 3.79 (s, 6H), 3.93 (s, 3H), 4.01 (s, 3H), 6.84 (d, *J* = 8.8 Hz, 1H), 7.06 (m, 3H), 7.09 (d, *J* = 8.8 Hz, 1H), 9.96 (bs, 1H). ¹³C NMR (*d*₆-DMSO) δ: -0.45, 34.21, 55.67 (2C), 55.74, 60.10, 105.58, 106.71 (2C), 112.38, 116.45, 120.61 (2C), 124.00, 126.69, 129.18, 133.02, 141.91, 147.66, 152.59, 166.38, 186.43. MS (ESI): [M+1]⁺ = 539.3. Anal. calcd for C₂₂H₂₃IN₂O₆ C, 49.08; H, 4.31; N, 5.20; found: C, 48.89; H, 4.09; N, 5.03.

6.1.3.12. 2-Iodo-N-(2-(3,4-dimethoxybenzoyl)benzofuran-3-yl)acetamide (21). Following general procedure B, the crude residue purified by flash chromatography using ethyl acetate: petroleum ether 4:6 (v:v) as eluent furnished **21** as a white solid. Yield: 83%; mp 174–176 °C. ¹H NMR (CDCl₃) δ: 4.00 (s, 3H), 4.01 (s, 5H), 4.09 (s, 2H), 7.01 (d, *J* = 8.4 Hz, 1H), 7.31 (m, 1H), 7.53 (m, 2H), 7.77 (d, *J* = 2.0 Hz, 1H), 8.13 (dd, *J* = 8.4 and 2.0 Hz, 1H), 8.49 (d, *J* = 8.0 Hz, 1H), 11.2 (bs, 1H). ¹³C NMR (CDCl₃) δ: -1.15, 56.15, 56.26, 110.34, 111.98, 112.13, 120.85, 123.60, 125.34, 127.33, 127.40, 129.38, 129.78, 138.85, 149.12, 153.76, 154.48, 166.11, 184.06. MS (ESI): [M+1]⁺ = 466.6. Anal. calcd for C₁₉H₁₆INO₅ C, 49.05; H, 3.47; N, 3.01; found: C, 48.79; H, 3.28; N, 2.89.

6.1.3.13. 2-Iodo-N-(2-(4-methoxybenzoyl)benzofuran-3-yl)acetamide (22). Following general procedure B, the crude residue

purified by flash chromatography using ethyl acetate: petroleum ether 1.5:8.5 (v:v) as eluent furnished **22** as a white solid. Yield: 81%; mp 174–175 °C. ^1H NMR (CDCl_3) δ : 3.92 (s, 3H), 4.02 (s, 2H), 7.03 (d, $J = 8.8$ Hz, 2H), 7.32 (m, 1H), 7.52 (m, 2H), 8.31 (dd, $J = 8.4$ Hz, 2H), 8.49 (d, $J = 8.4$ Hz, 1H), 11.2 (bs, 1H). ^{13}C NMR (CDCl_3) δ : -1.09, 55.65, 112.18 (2C), 113.99 (2C), 120.87, 123.55, 127.36, 129.34, 129.72, 132.31, 132.46, 138.82, 154.49, 163.88, 166.12, 184.22. MS (ESI): $[\text{M}+1]^+ = 436.4$. Anal. calcd for $\text{C}_{18}\text{H}_{14}\text{INO}_4$ C, 49.68; H, 3.24; N, 3.22; found: C, 49.48; H, 3.13; N, 2.95.

6.1.3.14. N-(2-Benzoylbenzofuran-3-yl)-2-iodoacetamide (23). Following general procedure B, the crude residue purified by flash chromatography using ethyl acetate: petroleum ether 1.5:8.5 (v:v) as eluent furnished **23** as a white solid. Yield: 76%; mp 144–145 °C. ^1H NMR (d_6 -DMSO) δ : 4.00 (s, 2H), 7.39 (t, $J = 7.6$ Hz, 1H), 7.59 (m, 3H), 7.71 (m, 2H), 7.90 (d, $J = 8.0$ Hz, 1H), 8.02 (dd, $J = 8.2$ and 1.6 Hz, 2H), 10.7 (bs, 1H). ^{13}C NMR (CDCl_3) δ : -0.23, 112.44, 122.42, 123.48, 123.73, 126.81, 128.56 (2C), 129.02 (2C), 129.10, 133.04, 136.58, 140.46, 153.15, 166.88, 184.16. MS (ESI): $[\text{M}+1]^+ = 406.4$. Anal. calcd for $\text{C}_{17}\text{H}_{12}\text{INO}_3$ C, 50.39; H, 2.98; N, 3.46; found: C, 50.13; H, 2.79; N, 3.25.

6.2. Biological assays. Materials and methods

6.2.1. Cell lines and culture

The K562 human myeloid cell line was used in this study. K562 express the anti-apoptotic oncogene BCR-ABL and high levels of phosphorylated STAT5. Cell lines were grown in RPMI 1640 (Gibco Grand Island, NY, USA) containing 10% FCS (Gibco), 100 U/ml penicillin (Gibco), 100 $\mu\text{g}/\text{ml}$ streptomycin (Gibco), and 2 mM L-glutamine (Sigma Chemical Co., St. Louis, MO) in a 5% CO_2 atmosphere at 37 °C.

6.2.2. Cell growth inhibitory activity

Cytotoxicity was evaluated by the trypan blue dye exclusion test. To determine the growth inhibitory activity of the drugs tested, 2×10^5 cells were plated into 25 mm wells (Costar, Cambridge, UK) in 1 mL of complete medium and treated with different concentrations of each drug. After a 48 h incubation, the number of viable cells was determined and expressed as percent of control proliferation.

6.2.3. Apoptosis evaluation

Drug induced apoptosis and necrosis was determined morphologically after labeling the cells with acridine orange and ethidium bromide and by the annexin V detection test. In the morphological test, cells (2×10^5) were centrifuged ($300 \times g$) and the pellet was resuspended in 25 μL of the dye mixture. Ten microliters of the mixture was examined under oil immersion with a $100 \times$ objective using a fluorescence microscope. Live cells were determined by the uptake of acridine orange (green fluorescence) and exclusion of ethidium bromide (red fluorescence) stain. Live and dead apoptotic cells were identified by perinuclear condensation of chromatin stained by acridine orange (100 $\mu\text{g}/\text{mL}$) or ethidium bromide (100 $\mu\text{g}/\text{mL}$), and by the formation of apoptotic bodies. The percentage of apoptotic cells was determined after counting at least 300 cells. For the annexin V test, cells (1×10^6) were washed with PBS and centrifuged at $200 \times g$ for 5 min. Cell pellets were suspended in 100 μL of staining solution containing FITC-conjugated annexin V and propidium iodide (Annexin-V-Fluos Staining Kit, Roche Molecular Biochemicals, Mannheim, Germany) and incubated for 15 min at 20 °C: Annexin V positive cells were evaluated by flow cytometry (Becton–Dickinson).

6.2.4. Flow cytometry analysis of cell cycle and apoptosis

Cells were washed once in ice-cold PBS and resuspended at 1×10^6 per mL in a hypotonic fluorochrome solution containing propidium iodide (Sigma) 50 $\mu\text{g}/\text{mL}$ in 0.1% sodium citrate plus 0.03% (v/v) nonidet P-40 (Sigma). After a 30 min incubation, the fluorescence of each sample was analyzed as single-parameter frequency histograms using a FACScan flow cytometer (Becton–Dickinson, San Jose, CA). The distribution of cells in the cell cycle was determined using the ModFit LT program (Verity Software House, Inc.). Apoptosis was determined by evaluating the percentage of hypodiploid nuclei accumulated in the sub- G_1 peak after labeling with propidium iodide.

6.2.5. Flow cytometric evaluation of intracellular proteins

About 1×10^6 cells were washed twice with PBS (Sigma) and resuspended in 100 μL cytofix/cytoperm solution (Becton–Dickinson) at 4 °C. After 20 min the cells were washed twice with BD Perm/Wash™ buffer solution (Becton–Dickinson) and incubated with 20 μL of the specific fluorochrome(PE)-conjugated monoclonal antibody anti-p-STAT5 (Becton–Dickinson) at 4 °C. After 30 min the cells were washed twice and analyzed by flow cytometry. Alternatively, the cells were incubated with 2 μL PE-conjugated rat anti-mouse IgG1 monoclonal antibody (Becton–Dickinson) at 4 °C. After 30 min the cells were washed twice and analyzed by a FACScan flow cytometer (Becton–Dickinson).

6.2.6. Effects on tubulin polymerization and on colchicine binding to tubulin

To evaluate the effect of the compounds on tubulin assembly *in vitro* [55], varying concentrations of compounds were pre-incubated with 10 μM bovine brain tubulin in glutamate buffer at 30 °C and then cooled to 0 °C. After addition of 0.4 mM GTP (final concentration), the mixtures were transferred to 0 °C cuvettes in a recording spectrophotometer and warmed to 30 °C. Tubulin assembly was followed turbidimetrically at 350 nm. The IC_{50} was defined as the compound concentration that inhibited the extent of assembly by 50% after a 20 min incubation. The ability of the test compounds to inhibit colchicine binding to tubulin was measured as described [56], except that the reaction mixtures contained 1 μM tubulin, 5 μM [^3H]colchicine and 5 μM test compound.

Acknowledgments

The authors gratefully acknowledge Alberto Casolari for excellent technical assistance. The content of this paper is solely the responsibility of the authors and does not necessarily reflect the official views of the National Institutes of Health.

Appendix A. Supplementary data

Supplementary data related to this article can be found at <http://dx.doi.org/10.1016/j.ejmech.2015.11.022>.

References

- [1] B.J. Druker, M. Talpaz, D.J. Resta, B. Peng, E. Buchdunger, J.M. Ford, N.B. Lydon, H. Kantarjian, R. Capdeville, S. Ohno-Jones, C.L. Sawyers, Efficacy and safety of a specific inhibitor of the BCR-ABL tyrosine kinase in chronic myeloid leukemia, *N. Engl. J. Med.* 344 (2001) 1031–1037.
- [2] A. Quintas-Cardama, H. Kantarjian, J. Cortes, Flying under the radar: the new wave of BCR-ABL inhibitors, *Nat. Rev. Drug Discov.* 6 (2007) 834–848.
- [3] M. Tolomeo, F. Dieli, N. Gebbia, D. Simoni, Tyrosine kinase inhibitors for the treatment of chronic myeloid leukemia, *Anticancer Agents Med. Chem.* 9 (2009) 853–863.
- [4] M.E. Gorre, M. Mohammed, K. Ellwood, N. Hsu, R. Paquette, P.N. Rao, C.L. Sawyers, Clinical resistance to STI-571 cancer therapy caused by BCR-ABL gene mutation or amplification, *Science* 293 (2001) 876–880.
- [5] J.A. Engelman, J. Settleman, Acquired resistance to tyrosine kinase inhibitors

- during cancer therapy, *Curr. Opin. Genet. Dev.* 18 (2008) 73–79.
- [6] R. Barouch-Bentov, Mechanisms of drug-resistance in kinases, *Expert Opin. Investig. Drugs* 2 (2011) 153–208.
- [7] S. Chu, L. Li, H. Singh, R. Bhatia, BCR-tyrosine 177 plays an essential role in Ras and Akt activation and in human hematopoietic progenitor transformation in chronic myelogenous leukemia, *Cancer Res.* 67 (2007) 7045–7053.
- [8] M. Horita, E.J. Andreu, A. Benito, C. Arbona, C. Sanz, I. Benet, F. Prosper, J.L. Fernandez-Luna, Blockade of the Bcr-Abl kinase activity induces apoptosis of chronic myelogenous leukemia cells by suppressing signal transducer and activator of transcription 5-dependent expression of Bcl-xL, *J. Exp. Med.* 191 (2000) 977–984.
- [9] M. Cirinna, R. Trotta, P. Salomoni, P. Kossev, M. Wasik, D. Perrotti, B. Calabretta, Bcl-2 expression restores the leukemogenic potential of a BCR/ABL mutant defective in transformation, *Blood* 96 (2000) 3915–3921.
- [10] R.R. Hoover, M.J. Gerlach, E.Y. Koh, G.Q. Daley, Cooperative and redundant effects of STAT5 and Ras signaling in BCR/ABL transformed hematopoietic cells, *Oncogene* 20 (2001) 5826–5835.
- [11] F. Gesbert, J.D. Griffin, Bcr/Abl activates transcription of the Bcl-X gene through STAT5, *Blood* 96 (2000) 2269–2276.
- [12] R.P. de Groot, J.A. Raaijmakers, J.W. Lammers, L. Koenderman, STAT5-dependent cyclinD1 and Bcl-xL expression in Bcr-Abl-transformed cells, *Mol. Cell Biol. Res. Commun.* 3 (2000) 299–305.
- [13] C. Sillaber, F. Gesbert, D.A. Frank, M. Sattler, J.D. Griffin, STAT5 activation contributes to growth and viability in Bcr/Abl-transformed cells, *Blood* 95 (2000) 2118–2125.
- [14] R.P. De Groot, J.A.M. Raaijmakers, J.-J. Lammers, R. Jove, L. Koenderman, STAT5 activation by Bcr-Abl contributes to transformation of K562 leukemia cells, *Blood* 94 (1999) 1108–1112.
- [15] M. Basákiewicz-Masiuk, B. Machaliński, The role of the STAT5 proteins in the proliferation and apoptosis of the CML and AML cells, *Eur. J. Haematol.* 72 (2004) 420–429.
- [16] D. Ye, N. Wolff, L. Li, S. Zhang, R.L. Ilaria Jr., STAT5 signaling is required for the efficient induction and maintenance of CML in mice, *Blood* 107 (2006) 4917–4925.
- [17] K. Spiekermann, M. Pau, R. Schwab, K. Schmieja, S. Franzrahe, W. Hiddemann, Constitutive activation of STAT3 and STAT5 is induced by leukemic fusion proteins with protein tyrosine kinase activity and is sufficient for transformation of hematopoietic precursor cells, *Exp. Hematol.* 30 (2002) 262–271.
- [18] C. Lacout, D.F. Pisani, M. Tulliez, F.M. Gachelin, W. Vainchenker, J.L. Villeval, JAK2V617F expression in murine hematopoietic cells leads to MPD mimicking human PV with secondary myelofibrosis, *Blood* 108 (2006) 1652–1660.
- [19] G. Wernig, T. Mercher, R. Okabe, R.L. Levine, B.H. Lee, D.G. Gilliland, Expression of Jak2V617F causes a polycythemia vera-like disease with associated myelofibrosis in a murine bone marrow transplant model, *Blood* 107 (2006) 4274–4281.
- [20] V. Gouilleux-Gruart, F. Debierre-Grockiego, F. Gouilleux, J.C. Capiod, J.F. Claisse, J. Delobel, L. Prin, Activated Stat related transcription factors in acute leukemia, *Leuk. Lymphoma* 28 (1997) 83–88.
- [21] V. Gouilleux-Gruart, F. Gouilleux, C. Desaint, J.C. Claisse, J.F. Capiod, J. Delobel, R. Weber-Nordt, I. Dusanter-Fourt, F. Dreyfus, B. Groner, L. Prin, STAT-related transcription factors are constitutively activated in peripheral blood cells from acute leukemia patients, *Blood* 87 (1996) 1692–1697.
- [22] R.M. Weber-Nordt, C. Egen, J. Wehinger, W. Ludwig, V. Gouilleux-Gruart, R. Mertelsmann, J. Finke, Constitutive activation of STAT proteins in primary lymphoid and myeloid leukemia cells and in Epstein-Barr virus (EBV)-related lymphoma cell lines, *Blood* 88 (1996) 809–816.
- [23] T. Nosaka, T. Kawashima, K. Misawa, K. Ikuta, A.L. Mui, T. Kitamura, STAT5 as a molecular regulator of proliferation, differentiation and apoptosis in hematopoietic cells, *EMBO J.* 18 (1999) 4754–4765.
- [24] T. Bowman, R. Garcia, J. Turkson, R. Jove, STATs in oncogenesis, *Oncogene* 19 (2000) 2474–2488.
- [25] J. Bromberg, Stat proteins and oncogenesis, *J. Clin. Investig.* 109 (2002) 1139–1142.
- [26] J. Turkson, R. Jove, STAT proteins: novel molecular targets for cancer drug discovery, *Oncogene* 19 (2000) 6613–6626.
- [27] J. Bromberg, J.E. Darnell, The role of STATs in transcriptional control and their impact on cellular function, *Oncogene* 19 (2000) 2468–2473.
- [28] S.R. Walker, M. Xiang, D.A. Frank, Distinct roles of STAT3 and STAT5 in the pathogenesis and targeted therapy of breast cancer, *Mol. Cell. Endocrinol.* 382 (2014) 616–621.
- [29] K. Shuai, J. Halpern, J. Ten Hoeve, X. Rao, C.L. Sawyers, Constitutive activation of STAT5 by the BCR-ABL oncogene in chronic myelogenous leukemia, *Oncogene* 13 (1996) 247–254.
- [30] D.A. Frank, L. Varticovski, BCR/abl leads to the constitutive activation of Stat proteins, and shares an epitope with tyrosine phosphorylated Stats, *Leukemia* 10 (1996) 1724–1730.
- [31] H. Yu, R. Jove, The STATs of cancer—new molecular targets come of age, *Nat. Rev. Cancer* 4 (2004) 97–105.
- [32] D.A. Frank, STAT signaling in cancer: insights into pathogenesis and treatment strategies, *Cancer Treat. Res.* 115 (2003) 267–291.
- [33] J.N. Ihle, The Stat family in cytokine signaling, *Curr. Opin. Cell Biol.* 13 (2001) 211–217.
- [34] D.E. Levy, J.E. Darnell Jr., STATs: transcriptional control and biological impact, *Nat. Rev. Mol. Cell Biol.* 2 (2002) 651–662.
- [35] W. Warsch, C. Walz, V. Sexl, JAK of all trades: JAK2-STAT5 as novel therapeutic targets in BCR-ABL1+ chronic myeloid leukemia, *Blood* 122 (2013) 2167–2175.
- [36] A.A. Kumaraswamy, A. Todic, D. Resetca, M.D. Minden, P.T. Gunning, Inhibitors of Stat5 protein signaling, *Med. Chem. Commun.* 3 (2012) 22–27.
- [37] J. Muller, B. Sperl, W. Reindl, A. Kiessling, T. Berg, Discovery of chromone-based inhibitors of the transcription factor Stat5, *Chem. Bio. Chem.* 9 (2008) 723–727.
- [38] E.A. Nelson, S.R. Walker, M. Xiang, E. Weisberg, M. Bar-Natan, R. Barrett, S. Liu, S. Kharbanda, A.L. Christie, M. Nicolais, J.D. Griffin, R.M. Stone, A.L. Kung, D.A. Frank, The STAT5 inhibitor pimozone displays efficacy in models of acute myelogenous leukemia driven by FLT3 mutations, *Blood* 117 (2011) 3421–3429.
- [39] B.D. Page, H. Khoury, R.C. Laister, S. Fletcher, M. Vellozo, A. Manzoli, P. Yue, J. Turkson, M.D. Minden, P.T. Gunning, Small molecule STAT5-SH2 domain inhibitors exhibit potent antileukemia activity, *J. Med. Chem.* 55 (2012) 1047–1055.
- [40] A.A. Kumaraswamy, A.M. Lewis, M. Geletu, A. Todic, D.B. Diaz, X.R. Cheng, C.E. Brown, R.C. Laister, D. Muench, K. Kerman, H.L. Grimes, M.D. Minden, P.T. Gunning, Nanomolar-potency small molecule inhibitor of STAT5 protein, *ACS Med. Chem. Lett.* 5 (2014) 1202–1206.
- [41] R. Ronchini, D. Simoni, R. Romagnoli, R. Baruchello, P. Marchetti, C. Costantini, S. Fochi, G. Padroni, S. Grimaudo, R.M. Pipitone, M. Meli, M. Tolomeo, Inhibition of activated STAT5 in Bcr/Abl expressing leukemia cells with new pimozone derivatives, *Bioorg. Med. Chem. Lett.* 24 (2014) 4568–4574.
- [42] N. Elumalai, A. Berg, K. Natarajan, A. Scharow, T. Berg, Nanomolar inhibitors of the transcription factor STAT5b with high selectivity over STAT5a, *Angew. Chem. Int. Ed. Engl.* 54 (2015) 4758–4763.
- [43] R. Romagnoli, P.G. Baraldi, T. Sarkar, M.D. Carrion, O. Cruz-Lopez, C. Lopez Cara, M. Tolomeo, S. Grimaudo, A. Di Cristina, M.R. Pipitone, J. Balzarini, R. Gambari, I. Lampronti, R. Saletti, A. Brancale, E. Hamel, Synthesis and biological evaluation of 2-(3',4',5'-trimethoxybenzoyl)-3-N,N-dimethylamino benzo[b]furan derivatives as inhibitors of tubulin polymerization, *Bioorg. Med. Chem.* 16 (2008) 8419–8426.
- [44] S. Grimaudo, M. Meli, A. Di Cristina, A. Ferro, M.R. Pipitone, R. Romagnoli, D. Simoni, F. Dieli, M. Tolomeo, The new iodoacetamidobenzofuran derivative TR120 decreases STAT5 expression and induces antitumor effects in imatinib-sensitive and imatinib-resistant BCR-ABL-expressing leukemia cells, *Anti-cancer Drugs* 24 (2013) 384–393.
- [45] K. Gaukroger, J.A. Hadfield, N.J. Lawrence, S. Nlan, A.T. McGown, Structural requirements for the interaction of combretastatins with tubulin: how important is the trimethoxy unit? *Org. Biomol. Chem.* 1 (2003) 3033–3037.
- [46] For the preparation of compounds 2–4, 16, 19 and 20 see R. Romagnoli, P.G. Baraldi, M.D. Carrion, C. Lopez-Cara, A. Casolari, E. Hamel, E. Fabbri, R. Gambari, Synthesis and evaluation of haloacetyl, α -bromoacryloyl and nitroxyacetyl benzo[b]furan and benzo[b]thiophene derivatives as potent antiproliferative agents against leukemia L1210 and K562 cells, *Lett. Drug Des. Discov.* 7 (2010) 476–486;
- a Compounds 17 and 18 were synthesized following the procedure reported in the article R. Romagnoli, P.G. Baraldi, C. Lopez-Cara, D. Preti, M. Aghazadeh Tabrizi, J. Balzarini, B. Bassetto, A. Brancale, X.-H. Fu, Y. Gao, J. Li, S.-Z. Zhang, E. Hamel, R. Bortolozzi, G. Basso, G. Viola, Concise synthesis and biological evaluation of 2-aryloxy-5-amino benzo[b]thiophene derivatives as a novel class of potent antimetabolic agents, *J. Med. Chem.* 56 (2013) 9296–9309.
- [47] For the preparation of 2-(3',4',5'-trimethoxybenzoyl)benzo[b]furan derivatives 24–31 see R. Romagnoli, P.G. Baraldi, C. Lopez Cara, O. Cruz-Lopez, M.D. Carrion, M. Kimatrai Salvador, J. Bermejo, S. Estévez, F. Estévez, J. Balzarini, A. Brancale, A. Ricci, L. Chen, J. Gwan Kim, E. Hamel, Synthesis and antitumor molecular mechanism of agents based on amino 2-(3',4',5'-trimethoxybenzoyl)benzo[b]furan: inhibition of tubulin and induction of apoptosis, *ChemMedChem* 6 (2011) 1841–1853;
- a For the synthesis of 2-(3',4',5'-trimethoxybenzoyl)-3-aminoindoles 32–34 see R. Romagnoli, P.G. Baraldi, T. Sarkar, M.D. Carrion, C. Lopez-Cara, O. Cruz-Lopez, D. Preti, M.A. Tabrizi, M. Tolomeo, S. Grimaudo, A. Di Cristina, N. Zonta, J. Balzarini, A. Brancale, H.P. Hsieh, E. Hamel, Synthesis and biological evaluation of 1-methyl-2-(3' 4',5'-trimethoxybenzoyl)-3-amino indoles as a new class of antimetabolic agents and tubulin inhibitors, *J. Med. Chem.* 51 (2008) 1464–1468;
- b 2-Aryloxy-3-aminobenzo[b]furan derivatives 35–37 were synthesized following the procedure reported in the article S. Radl, P. Hezky, P. Konvicka, I. Kreici, Synthesis and analgesic activity of some substituted 1-benzofurans and 1-benzothiophenes, *Collect. Czechoslov. Chem. Commun.* 7 (2000) 1093–1108.
- [48] I. Matsumura, T. Kitamura, H. Wakao, H. Tanaka, K. Hashimoto, C. Albanese, J. Downward, R.G. Pestell, Y. Kanakura, Transcriptional regulation of the cyclin D1 promoter by STAT5: its involvement in cytokine-dependent growth of hematopoietic cells, *EMBO J.* 18 (1999) 1367–1377.
- [49] F. Gesbert, J.D. Griffin, Bcr/Abl activates transcription of the Bcl-X gene through STAT5, *Blood* 96 (2000) 2269–2276.
- [50] T.L. Kubota, M. Miyauchi, K. Miura, G. Hirokawa, A. Awaya, N. Miyasaka, Y. Kurosawa, Y. Kanai, K. Maruyama, Upregulation of nucleobindin expression in human-activated lymphocytes and non-Hodgkin's lymphoma, *Pathol. Int.* 48 (1998) 22–28.
- [51] J.W. Lee, H.Y. Chung, L.A. Ehrlich, D.F. Jelinek, N.S. Callander, G.D. Roodman, S.J. Choi, IL-3 expression by myeloma cells increases both osteoclast formation and growth of myeloma cells, *Blood* 103 (2004) 2308–2315.

- [52] M. Lopez-Perez, E.P. Salazar, A role for the cytoskeleton in STAT5 activation in MCF7 human breast cancer cells stimulated with EGF. *Int. J. Biochem. Cell Biol.* 6 (2006) 1716–1728.
- [53] E.L. Gleason, J.C. Hogan, J.M. Stephens, Stabilization, not polymerization, of microtubules inhibits the nuclear translocation of STATs in adipocytes. *Biochem. Biophys. Res. Commun.* 325 (2004) 716–718.
- [54] C. Moser, S.A. Lang, A. Mori, C. Hellerbrand, H.J. Schlitt, E.K. Geissler, W.E. Fogler, O. Stoeltzing, ENMD-1198, a novel tubulin-binding agent reduces HIF-1 α and STAT3 activity in human hepatocellular carcinoma (HCC) cells, and inhibits growth and vascularization in vivo. *BMC Cancer* 8 (2008) 206–217.
- [55] E. Hamel, Evaluation of antimitotic agents by quantitative comparisons of their effects on the polymerization of purified tubulin. *Cell Biochem. Biophys.* 38 (2003) 1–21.
- [56] P. Verdier-Pinard, J.-Y. Lai, H.-D. Yoo, J. Yu, B. Marquez, D.G. Nagle, M. Nambu, J.D. White, J.R. Falck, W.H. Gerwick, B.W. Day, E. Hamel, Structure-activity analysis of the interaction of curacin A, the potent colchicine site antimitotic agent, with tubulin and effects of analogs on the growth of MCF-7 breast cancer cells. *Mol. Pharmacol.* 53 (1998) 62–76.